Article

Current Biology

Ventro-dorsal Hippocampal Pathway Gates Novelty-Induced Contextual Memory Formation

Graphical Abstract

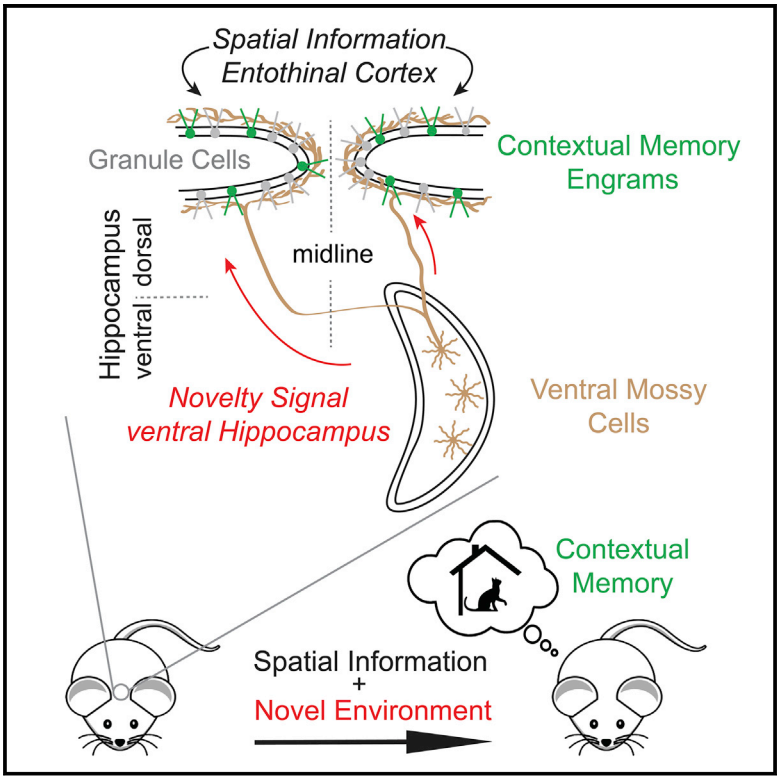

Highlights

- Mossy cells in ventral hilus directly excite granule cells in dorsal hippocampus
- Activity of ventral mossy cells positively correlates with environmental novelty
- Inhibiting ventral mossy cells disrupts novelty-induced contextual fear memory
- Exciting ventral mossy cells enhances contextual memory in a familiar environment

Authors

Felipe Fredes, Maria Alejandra Silva, Peter Koppensteiner, Kenta Kobayashi, Maximilian Joesch, Ryuichi Shigemoto

Correspondence

ffredes@dandrite.au.dk (F.F.), ryuichi.shigemoto@ist.ac.at (R.S.)

In Brief

Novelty facilitates memory formation. Fredes et al. show that mossy cells in the ventral dentate gyrus detect environmental novelty. This information is conveyed to dorsal dentate granule cells and is necessary for novelty-induced contextual memory formation. Conversely, activating this pathway enhances contextual memory in a familiar environment.

Fredes et al., 2021, Current Biology *31*, 1–14
January 11, 2021
https://doi.org/10.1016/j.cub.2020.09.074

CellPress

Please cite this article in press as: Fredes et al., Ventro-dorsal Hippocampal Pathway Gates Novelty-Induced Contextual Memory Formation, Current Biology (2020), https://doi.org/10.1016/j.cub.2020.09.074

Current Biology

CellPress
OPEN ACCESS

Article

Ventro-dorsal Hippocampal Pathway Gates Novelty-Induced Contextual Memory Formation

Felipe Fredes,[1,2,*] Maria Alejandra Silva,[1] Peter Koppensteiner,[1] Kenta Kobayashi,[3] Maximilian Joesch,[1,4] and Ryuichi Shigemoto[1,4,5,*]

[1]Institute of Science and Technology Austria, Am Campus 1, 3400 Klosterneuburg, Austria
[2]Department of Biomedicine, Aarhus University, Ole Worms Alle 6, Building 1182, 8000 Aarhus C, Denmark
[3]Section of Viral Vector Development, National Institute for Physiological Sciences, Myodaiji, Okazaki, Japan
[4]Senior author
[5]Lead Contact
*Correspondence: ffredes@dandrite.au.dk (F.F.), ryuichi.shigemoto@ist.ac.at (R.S.)
https://doi.org/10.1016/j.cub.2020.09.074

SUMMARY

Novelty facilitates memory formation and is detected by both the dorsal and ventral hippocampus. Although dentate granule cells (GCs) in the dorsal hippocampus are known to mediate the formation of novelty-induced contextual memories, the required pathways and mechanisms remain unclear. Here we demonstrate that a powerful excitatory pathway from mossy cells (MCs) in the ventral hippocampus to dorsal GCs is necessary and sufficient for driving dorsal GC activation in novel environment exploration. *In vivo* Ca^{2+} imaging in freely moving mice indicated that this pathway relays environmental novelty. Furthermore, manipulation of ventral MC activity bidirectionally regulates novelty-induced contextual memory acquisition. Our results show that ventral MC activity gates contextual memory formation through an intra-hippocampal interaction activated by environmental novelty.

INTRODUCTION

Contextual memory is formed by a combination of multiple sensory stimuli and can be tightly associated with context-specific episodes. This association is often facilitated by various types of novelty signals.[1] The detection of such novelty signals involves the hippocampus,[2,3] especially its ventral moiety[4] and its human homolog (anterior hippocampus),[5] whereas acquisition, retrieval, and extinction of contextual memory involve the dorsal hippocampus.[6–8] The anatomical and functional distinction between the dorsal and ventral hippocampus has been extensively investigated,[8–11] but, see,[12] the interactions between the ventral and dorsal hippocampal moieties remain elusive. Granule cells (GCs) in the dorsal dentate gyrus (DG) increase their activity during novel environment exploration,[13,14] forming changes in the population activity of GCs bearing correlates of contextual memory engrams.[15–20] They receive major excitatory inputs from the entorhinal cortex in the outer two-thirds of the molecular layer (ML). In contrast, another massive excitatory synaptic connection is made in the inner one-third of ML by mossy cells (MCs) located in the dorsal and ventral hilus[21–23] (Figures 1A and 1B). Both of these excitatory inputs also innervate interneurons in the hilus[24,25] and provide a strong di-synaptic inhibition to GCs sparsifying the output of DG.[26–28] Furthermore, entorhinal inputs to GCs have not been observed to provide strong environmental novelty signals,[29,30] although the data on this topic are quite limited, and it remains an open question as to whether the entorhinal cortex contains such novelty signals. Thus, the mechanism underlying the initiation of GCs firing that leads to the formation of contextual memories remains unclear. Because novelty signals increased c-Fos+ MCs preferentially in the ventral hippocampus,[31,32] it has been hypothesized that the extensive projections of ventral MCs to the dorsal DGs could convey novelty signals to dorsal GCs,[24] though the same novelty signals failed to increase c-Fos+ dorsal GCs.[32] Here we present functional and behavioral evidence demonstrating that environmental novelty detected by ventral MCs is relayed to dorsal GCs and that ventral MC activation is an essential regulator of contextual memory formation.

We show that in contrast to dorsal MC projections, ventral MC projections provide a powerful net excitatory effect on dorsal GCs. Ca^{2+} imaging in freely moving mice indicates that the population activity of both ventral MCs and dorsal GCs is directly linked with the level of environmental novelty—it decreases with familiarization and rebounds when animals explore a new environment again. Furthermore, we show that inhibiting this ventro-dorsal pathway abolishes the formation of contextual memory. Finally, although animals are unable to form contextual memory when conditioned in a familiar environment, chemogenetic reactivation of ventral MCs is sufficient to rescue the formation of contextual memory in a familiar environment. Thus, our data unveil a mechanistic link between novelty detection and contextual memory formation by direct interaction of the ventral and dorsal hippocampus.

RESULTS

Viral Vector Approach to Target Ventral MCs

MCs in the ventral, but not the dorsal region, of the hippocampus have been shown to be calretinin-positive (Calb2+),[22,23,33]

Please cite this article in press as: Fredes et al., Ventro-dorsal Hippocampal Pathway Gates Novelty-Induced Contextual Memory Formation, Current Biology (2020), https://doi.org/10.1016/j.cub.2020.09.074

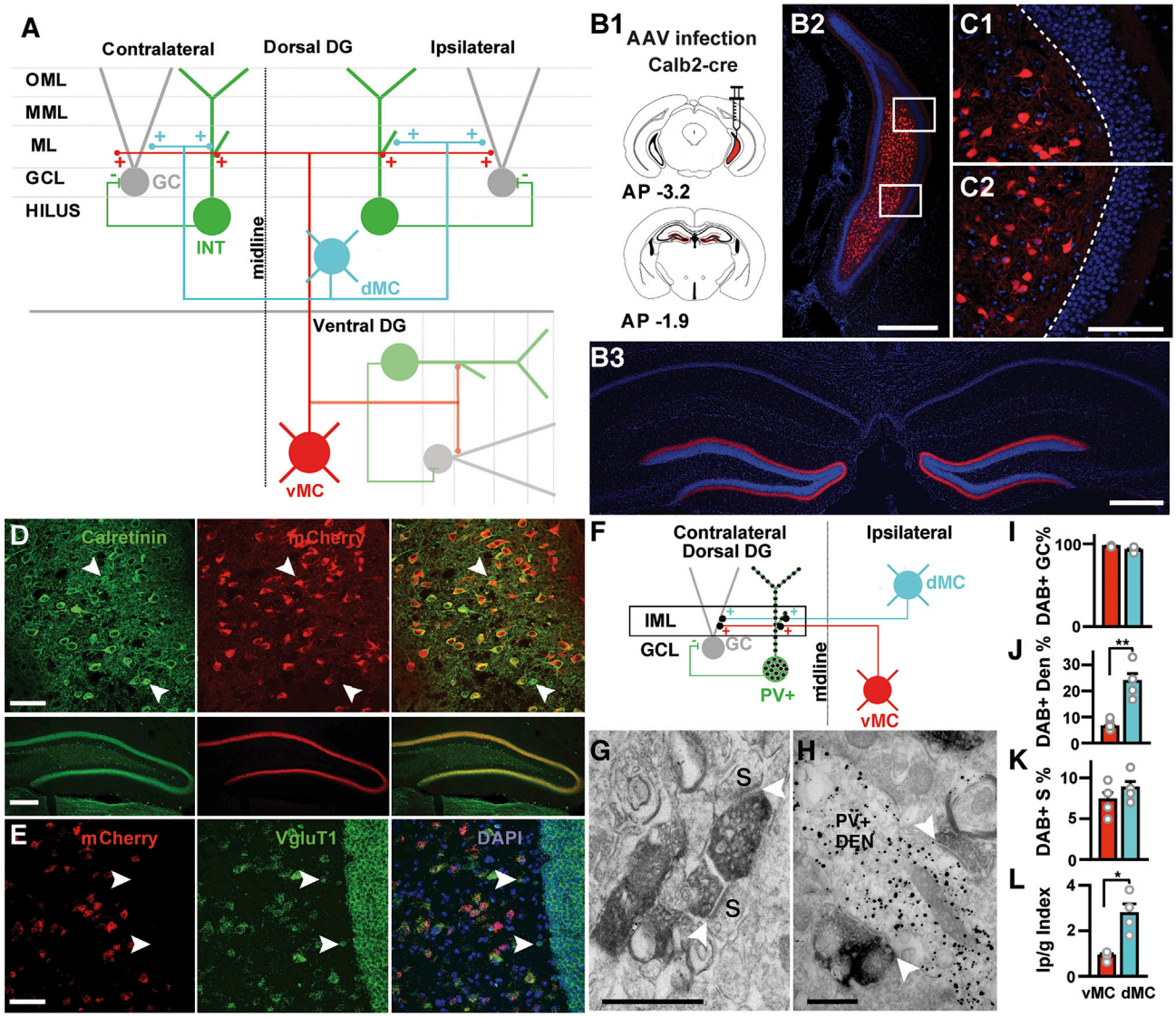

Figure 1. Ventral MC's Bilateral Projections to the Dorsal DG Contact Mostly GC Spines

(A) Schematic representation of connectivity between dorsal MCs (cyan) and ventral MCs (red) with interneurons (green) and GCs (gray). IML, inner ML; MML, medial ML; OML, outer ML; GCL, GC layer.

(B) Cre-dependent mCherry expression in the ventral hilus and dorsal DG after injection of AAV_5-hSyn-DIO-mCherry into the ventral hilus of a Calb2-cre mouse. Schematic of unilateral injection (B1). AP, antero-posterior coordinates with respect to bregma. Ventral (B2) and dorsal (B3) hippocampal example images. DAPI (4',6'-diamino-2-phenylindole) labels cell nuclei. Scale bars, 500 μm.

(C) Close-ups of mCherry-positive cells in the ventral hilus; dotted line highlights the boundary between hilus and GC layer. No cells were ever found in the GC layer three weeks after infection. Scale bar, 200 μm.

(D) mCherry-expressing cells in the ventral hilus and their terminals in the dorsal DG are Calb2 immuno-positive. White arrowheads show Calb2-positive cells that do not express mCherry. Scale bar, 100 μm (upper panel); 200 μm (middle panel).

(E) Fluorescent *in situ* hybridization for mCherry and vGluT1. Scale bar, 50 μm. White arrows indicate vGluT1-positive cells negative for mCherry.

(F) Schematic representation of the electron-microscopic connectivity experiment. Contralateral dorsal MCs (cyan) or ventral MCs axonal projections (red) were labeled with DAB (dark synapses) and PV+ interneurons (green) with immunogold particles (black dots) in the dorsal DG. The relative synaptic connection in the IML between GCs (gray) and PV+ interneurons were quantified anatomically (box).

(G) DAB-labeled terminals from ventral MCs synapsing (white arrowheads) onto GC spines (s). Scale bar, 500 nm.

(H) Two DAB-labeled terminals from dorsal MCs making synaptic contacts (white arrowheads) with a single PV+ dendritic shaft (PV+ DEN) immunolabeled with gold particles. Scale bar, 500 nm.

(I) Quantification of DAB-labeled synapses made on GC spines (in percentage of all DAB-labeled synapses) by ventral MCs (vMCs) and dorsal MCs (dMCs). Mean + SE, n = 4 animals.

(legend continued on next page)

Please cite this article in press as: Fredes et al., Ventro-dorsal Hippocampal Pathway Gates Novelty-Induced Contextual Memory Formation, Current Biology (2020), https://doi.org/10.1016/j.cub.2020.09.074

opening the possibility to target and manipulate ventral MCs by using Calb2-cre mice. Calretinin, however, has also been shown to be expressed in newly born GCs, most abundantly located in the hilus at postnatal day 16[34] as well as in interneurons.[35] Thus, we tested if the intersection of adeno-associated virus (AAV) infection in adult Calb2-cre mice could narrow down the expression pattern to ventral MCs. After injection of AAV with cre-dependent expression of mCherry into the ventral hilus of a Calb2-cre mouse (Figure 1B subpanel 1), we identified a dense and bilateral projection to the inner ML that extensively spanned the whole dorso-ventral hippocampal axis with no other distinct projections in the hippocampus (Figures 1B [subpanel 3] and S1A). The vast majority of mCherry-expressing cells located in the ventral one-third of the hilus were Calb2+ (93%, n = 175 cells) as expected (Figure 1D). Their terminals in the dorsal DG were Calb2+ as well (Figure 1D). *In situ* hybridization showed that all the mCherry-expressing cells are vGluT1+ (n = 67 cells, Figure 1E), confirming that they are glutamatergic and that interneurons did not express our construct. Next, we tested if our approach targets newly born GCs. Newly born GCs migrate from the sublaminar to the GC layer in the first week after cell division and start extending their axonal and dendritic processes to the hilus and ML, respectively, in the second week.[36] We found no cells in the GC layer three weeks after infection (Figure 1C), consistent with a recent report showing a high sensitivity to AAV-induced cell death specific for immature dentate GCs.[37] Only a small number of pyramidal cells in the CA3 area (7% of all labeled cells) expressed mCherry (Figures S1A and S1B). These results indicate that the vast majority of targeted cells in our approach are ventral MCs.

PV+ Interneurons in the Dorsal DG Receive Strong Excitatory Input from Dorsal but Not Ventral MCs

Given that both dorsal and ventral MCs project to the dorsal inner ML and that optogenetic stimulation of dorsal MC axons primarily drives interneuron firing,[27] we compared the postsynaptic targets of ventral and dorsal MCs in the dorsal inner ML. The majority of interneuron dendrites in the ML originate from parvalbumin-positive (PV+) cells (85%, Figures S2H–S2J). These are robustly activated by dorsal MCs[27] and have the highest probability of innervating GCs among all interneurons, 2.5 and 10 times higher than cholecystokinin (CCK) and somatostatin (SOM)-positive cells, respectively.[38] Thus, among all interneurons, PV+ interneurons have the strongest direct inhibitory influence on GC activity. Therefore, we quantified by electron microscopy the numbers of asymmetrical (glutamatergic) synapses arising from ventral or dorsal MCs onto dendritic shafts of PV+ interneurons and those onto GC spines within the inner ML of dorsal DG (Figures 1F–1L; also see STAR Methods). To visualize MC terminals, we expressed a membrane-bound fluorescent protein in ventral and dorsal MCs by AAV injection into the contralateral hilus (Figures 1F, S2A, and S2B) and immunolabeled their terminals with diaminobenzidine (DAB) (Figures 1G, 1H, and S2C). Because a unilateral activation of ventral MCs has a similar effect on c-Fos expression in both contralateral and ipsilateral dorsal hippocampi (Figures S3A–S3E), we judge that the subsequent focus in the EM analysis can be generalized to the ipsilateral side too. Asymmetrical synapses made by DAB+ MC terminals were found on non-labeled GC spines (Figure 1G) and PV+ interneurons immunolabeled with gold particles (Figure 1H) in the inner ML. The vast majority of DAB+ terminals (96.7% for ventral MCs, 91.8% for dorsal MCs, Figure 1I; also see STAR Methods and Table S1) made synapses with GC spines consistent with previous findings,[21] whereas small numbers of DAB+ terminals with PV+ dendritic shafts (3.3% for ventral MCs, 8.2% for dorsal MCs, Figures 1G and 1H; Table S1). No PV+ spines (n = 20) made synapses with DAB+ terminals (Figures S2F and S2G). On the PV+ dendritic shafts, we found a higher percentage of DAB+ synapses made by dorsal (23.6%) than by ventral (6.22%) MCs (Figure 1J, p = 0.003), whereas no significant difference was observed on GC spines (Figure 1K). To control for any bias in MC infection rates, we also compare the relative innervation of PV+ interneurons normalized by that of GCs (Ip/g index, see STAR Methods) and found a 3.1-fold higher Ip/g value for dorsal than ventral MCs (Figure 1L, p = 0.006). Given that only a partial ipsilateral population of dorsal MCs were labeled in our experiments, the high percentage (23.6%) of labeled synapses on PV+ dendrites implies that the majority of excitatory inputs on these interneurons in the inner ML derive from dorsal MCs and only a minor population from ventral MCs. Thus, ventral MCs could exert a net excitatory effect on dorsal GCs in contrast to the net inhibitory effect exerted by dorsal MCs.[26,27]

Ventral MC Activity Is Required for Dorsal GC Activation during Novel Environment Exploration

To test whether the ventral MCs are capable of influencing the activation of dorsal GCs during novel environment exploration,[13,14] we modulated ventral MC activity and assayed changes in immediate early gene (c-Fos) expression, a proxy for neuronal activity, in the upper blade of dorsal GCs. We injected AAV expressing inhibitory designer receptors exclusively activated by designer drugs (DREADDs) (hM4Di) bilaterally into the ventral hilus of Calb2-cre mice. We confirmed that the vast majority of hM4Di-expressing cells were Calb2+ (95%, n = 134 cells). Three weeks later, these animals were injected with clozapine-N-oxide (CNO) intraperitoneally (intraperitoneally [i.p.], 3 mg/kg) 40 min before novel environment exploration (Figure 2A). We found a significant increase of c-Fos+ dorsal GCs in the upper blade after novel environment exploration in the control group expressing only mCherry (Figure 2H), consistent with the previous studies.[13,14] This increase was significantly attenuated in animals expressing hM4Di (Figures 2B, 2C, and 2H), mimicking the levels of c-Fos+ GCs observed in the home cage control condition (Figure 2H). The lower blade showed no significant difference in c-Fos expression between the mCherry and hM4Di groups (Figure S3G). In contrast, by using the same

(J) Quantification of dorsal and ventral MC synapses onto PV+ interneurons. Number of DAB-labeled synapses (in % of total synapses) onto PV+ dendrites (PV+ DENs) coming from either ventral or dorsal MCs. Mean + SE, n = 4 animals, **p = 0.003 (unpaired, two-tailed Student's t test).
(K) Number of DAB-labeled synapses (in percentage of total synapses) onto GC spines (S). Mean + SE, n = 4 animals.
(L) Index Ip/g (see STAR Methods) for ventral MCs and dorsal MCs, showing stronger innervation of PV+ dendrites by dorsal than ventral MCs. Mean + SE, n = 4 animals, p = 0.006 (unpaired, two tailed Student's t test). See also Figures S1, S2, and S3; Table S1.

Please cite this article in press as: Fredes et al., Ventro-dorsal Hippocampal Pathway Gates Novelty-Induced Contextual Memory Formation, Current Biology (2020), https://doi.org/10.1016/j.cub.2020.09.074

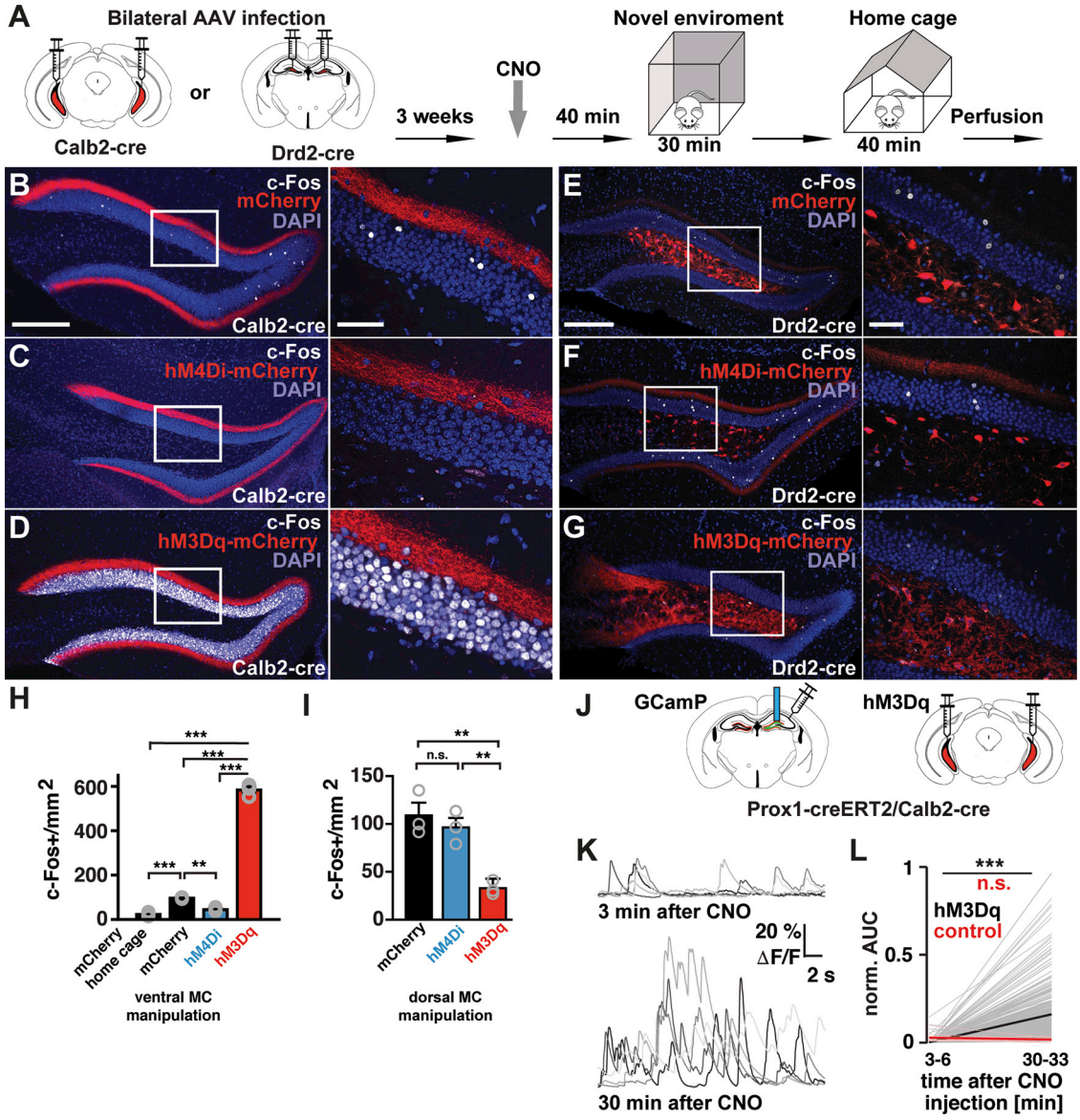

Figure 2. Strong Bidirectional Control of GC Activity by Ventral, but Not Dorsal Mossy Cells

(A) Schematic of experimental procedures where Calb2 or Drd2-cre mice were injected bilaterally into the ventral or dorsal hilus, respectively, with AAVs expressing mCherry, inhibitory DREADDs (hM4Di-mCherry), or excitatory DREADDs (hM3Dq-mCherry).

(B–D) Confocal images of the dorsal DG showing c-Fos+ neurons (white) from animals expressing mCherry (B), hM4Di-mCherry (C), or hM3Dq-mCherry (D) in ventral MCs. Higher magnification images of the boxed areas (left) are shown on the right. Scale bars, 200 μm (left); 100 μm (right).

(E–G) Representative images of the dorsal DG showing c-Fos+ neurons (white) from animals expressing mCherry (E), hM4Di-mCherry (F), or hM3Dq-mCherry (G) in dorsal MCs (red). White rectangles indicate the areas of the inset on the right. Note the decrease of c-Fos+ cells in the GC layer (G) in comparison with (E). Scale bars, 200 μm; inset, 50 μm.

(H and I) Quantification of c-Fos+ GCs in the upper blades of the dorsal DG from animals expressing mCherry, hM4Di-mCherry, or hM3Dq-mCherry in ventral MCs (H) or in dorsal MCs (I) after novel environment exploration (mean + SE, n = 3 animals per each group). An additional group of animals expressing mCherry in ventral MCs were perfused directly from the home cage after CNO injection ([H], mCherry home cage, n = 4 animals).

(H) For the ventral MC manipulation, significant differences were detected with one-way ANOVA ($F [3, 9] = 1031$, $p < 0.0001$). Tukey's multiple comparison test revealed that the number of c-Fos+ dorsal GCs significantly increased in animals expressing mCherry by novel environment exploration in comparison with the home cage control (***$p < 0.001$). This increase was attenuated in animals expressing hM4Di-mCherry in ventral MCs (**$p < 0.01$). In contrast, c-Fos+ dorsal GCs drastically increased in animals expressing hM3Dq-mCherry in ventral MCs (***$p < 0.001$).

(I) For the dorsal MC manipulation, significant differences were detected with one-way ANOVA ($F [2, 6] = 16, 90$, $p = 0.0034$). Tukey's multiple comparison test revealed a decrease in c-Fos+ cells in hM3Dq-mCherry group in comparison with mCherry (**$p = 0.0039$) and hM4Di-mCherry groups (**$p = 0.0095$).

(J) Schematic of experimental procedures where double transgenic mice Prox1-creERT2/Calb2-cre were injected bilaterally with AAV expressing hM3Dq-mCherry in the ventral hilus, and unilaterally with AAV expressing GCaMP6s in the dorsal DG. Later a GRIN lens (blue rod) was implanted above the injection site in the dorsal DG.

(legend continued on next page)

Please cite this article in press as: Fredes et al., Ventro-dorsal Hippocampal Pathway Gates Novelty-Induced Contextual Memory Formation, Current Biology (2020), https://doi.org/10.1016/j.cub.2020.09.074

procedure in animals expressing excitatory DREADDs (hM3Dq), we found a drastic increase in c-Fos+ dorsal GCs in comparison with the mCherry group in both upper (Figures 2B, 2D, and 2H) and lower blades (Figure S3G). Within the ventral DG of these animals, we also observed an increase of c-Fos+ GCs in comparison with mCherry-expressing animals, but the increment was weaker than that observed in the dorsal DG (Figure S3I). To examine whether the effects of inhibitory and excitatory DREADDs are specific to ventral but not dorsal MCs, we injected AAVs expressing mCherry, hM4Di-mCherry, or hM3Dq-mCherry bilaterally into the dorsal hilus of Drd2-cre mice expressing Cre in dorsal MCs[39] (Figures 2E–2G). Novel environment exploration after CNO injection showed a significant reduction of c-Fos+ dorsal GCs in hM3Dq- but not hM4Di-expressing animals (Figures 2E–2G and 2I), consistent with the net inhibitory effect on dorsal GCs exerted by dorsal MCs. The reduction in the lower blade (Figure S3H) was less robust than that in the upper blade (Figure 2I).

To corroborate the striking excitatory drive of ventral MCs *in vivo* and test whether it can activate dorsal GCs in a familiar environment, we recorded GC activity by Ca^{2+} imaging in freely behaving mice while simultaneously activating ventral MCs. We expressed hM3Dq bilaterally in the ventral MCs and the calcium indicator GCaMP6s unilaterally in the dorsal GCs in double transgenic mice Prox1-creERT2/Calb2-cre (Figure 2J). Through a GRIN lens implanted over the dorsal DG, we found the activity of dorsal GCs dramatically increased 30 min after CNO injection during familiar environment exploration (Figures 2K and 2L; Video S1). Altogether, these results indicate that the activation of long-range projections of ventral MCs has an excitatory net effect on dorsal GCs in contrast with the inhibitory effect of dorsal MC activation, consistent with our anatomical findings. The ventral MC activity can have a critical role in driving dorsal GC firing, mediating a direct flow of information from the ventral to the dorsal hippocampus.

Environmental Novelty Is a Strong Drive of Ventral MCs and Dorsal GCs

Exposure to novel objects induces preferential c-Fos expression in ventral in comparison with dorsal MCs, but not in GCs.[32] To examine whether ventral MCs and dorsal GCs are specifically activated in parallel by environmental novelty, we imaged the neuronal activity of these cells in freely exploring mice. First, we expressed GCaMP6s in dorsal GCs (Figures S4C and S4D) or ventral MCs (Figures S4G and S4H) by using Prox1-creERT2 or Calb2-cre mice, respectively. We then implanted a GRIN lens coupled to a head-mounted microendoscope to monitor activity-related calcium transients (Figures S4A and S4E). Animals explored a novel environment on day 1 for 20 min and then revisited the same environment for five additional days. Ca^{2+} imaging in these freely behaving animals revealed that both dorsal GCs (Figures 3A–3C, S4I, and S4O; Video S2) and ventral MCs (Figures 3F–3H, S4J, and S4P; Video S3) showed robust activity during novel environment exploration and decreased their activity during familiarization (Figures 3C, 3H, and S4Q). Moreover, the activity of both cell types immediately rebounded upon exposure to a new environment on day 6 (Figures 3C, 3H, S4I, S4J, S4O, and S4P; Videos S2 and S3). These changes in activity are driven in both cases mainly by changes in event sizes (Figures S4K–S4N). Because the increased locomotion in the novel environment could cause the activation of these neurons, and thus positively correlate with Ca^{2+} signals in GCs and MCs,[40,41] we examined the relationship between the speed of mouse movements and activity of dorsal GCs and ventral MCs in novel and familiar environments (Figures 3D, 3E, 3I, and 3J; Videos S2 and S3). Although the average locomotion speed showed a tendency to decrease through familiarization, this decrease was not significant (Figures 3D and 3I). Only dorsal GC activity tended to increase with locomotion speed in the novel (but not in familiar) environment (Figure 3E). However, no apparent increase of ventral MCs activity correlated with the speed was observed (Figure 3J), indicating that the increased activity of ventral MCs in the novel environment is not due to the increased locomotion.

To control for other behavioral influences on ventral MC activity, we designed an experiment in which the behavioral statistics remain constant (running on a wheel) across familiarization and observed twice as much average activity while running in the novel, in comparison with the familiar environment (Figure 3K). Although the correlated activity of ventral MCs and dorsal GCs does not mean causation, it suggests that the activity of ventral MCs could relay locomotion-independent novelty signals onto dorsal GCs on a population level. Finally, we tested if the foot shock provided during fear conditioning (see below) could serve as a novel signal and modulate ventral MC activity. To test this possibility, we performed Ca^{2+} imaging in ventral MCs and familiarized these animals in the conditioning cage, 10 min for six days. In accordance with previous results indicating that foot shocks do not influence dorsal GC activity,[15] ventral MCs were not reactivated by foot shock (Figures 3L and 3M). One limitation of these experiments is the damage introduced to the dendrites in the outer and middle ML (Figures S4C and S4D) due to the short working distance of our lens. Future experiments with longer working-distance lenses are necessary to clarify this confound (see Discussion). Overall, our results indicate that ventral MCs relay distinct information about environmental novelty to dorsal GCs.

Ventral MC Activity Is Required for Context-Memory Formation

Considering that dorsal GC activity is necessary for contextual memory formation,[17,18,42] we next examined whether ventral MC activity is required for context-dependent memory formation in fear conditioning (Figure 4). We expressed hM4Di bilaterally in the ventral MCs of Calb2-cre mice (Figure 4A) and injected CNO i.p. 40 min before fear conditioning (Figure 4B). These animals

(K) Examples of dorsal GC calcium transients before and after the effect of CNO. Note: the five most active cells are presented on the top traces, whereas a random set is selected in the bottom.

(L) Change in mean activity (AUC; see STAR Methods) for all recorded cells before and after the effect of CNO, 3–6 and 30–33 min after CNO injection, respectively (hM3Dq, n = 386 cells, $p < 0.001$ Wilcoxon signed-rank test; control, n = 15 cells, not significant). All experiments were performed after familiarization. Note that the reduced number of cells in the control condition reflects the normal sparse firing of dorsal GCs. See also Figure S3 and Video S1.

Please cite this article in press as: Fredes et al., Ventro-dorsal Hippocampal Pathway Gates Novelty-Induced Contextual Memory Formation, Current Biology (2020), https://doi.org/10.1016/j.cub.2020.09.074

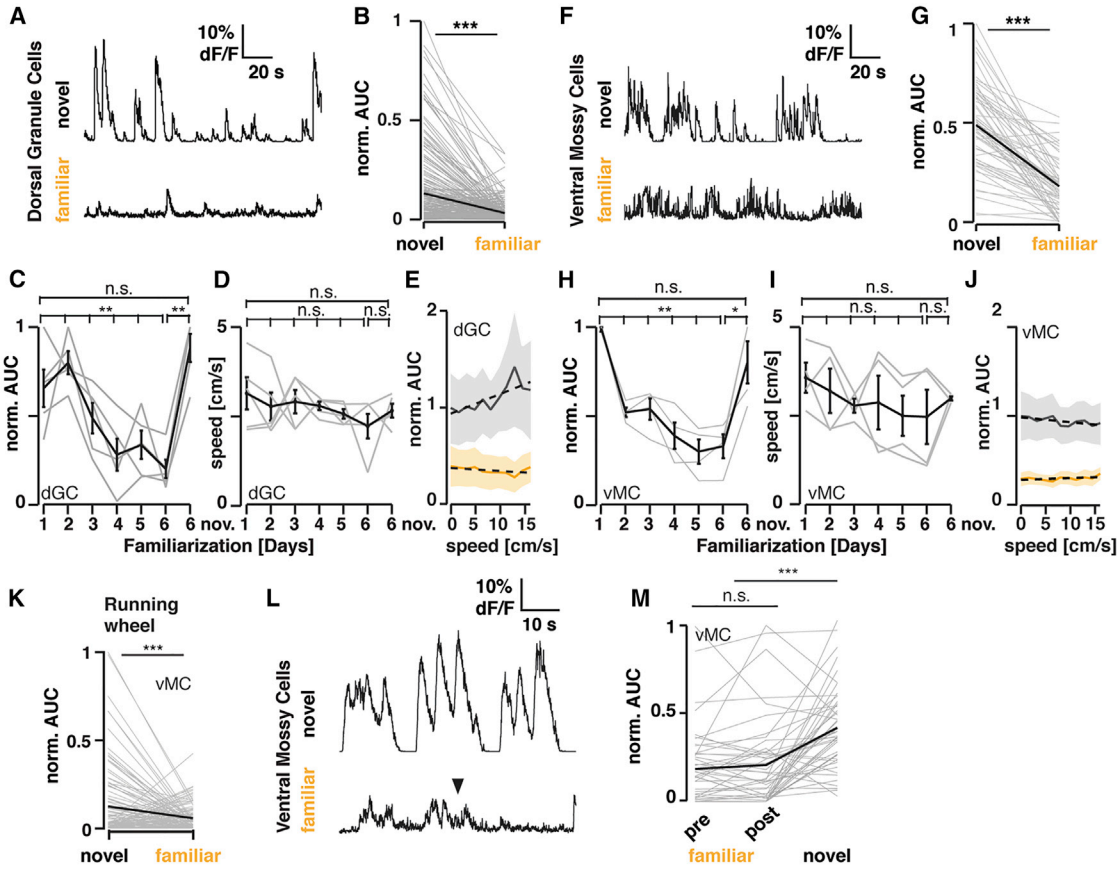

Figure 3. Ventral MCs and Dorsal GCs Are Robustly Activated by Novel Environment Exploration

(A) Example endoscope calcium imaging traces of the same dorsal GC during exploration of a novel and the same familiarized environment six days later (Prox1-creERT2 animals unilaterally injected with AAV9-hSyn-Flex-GCaMP6s into the dorsal DG).

(B) Changes in mean activity (AUC; see STAR Methods) for all recorded cells from the novel (day 1) to the same familiarized (day 6) environment (n = 229 cells, 5 animals, ***$p < 0.001$ Wilcoxon signed-rank test).

(C) Normalized average activity for an individual (gray trace) and the mean of all animals (black trace ± SEM) across familiarization and novel environment exploration (5 animals, **$p < 0.01$; Kruskal-Wallis test; Dunn's multiple comparison test revealed $p = 0.08$ between day 1 and day 6, and $p = 0.005$ between day 2 and day 6).

(D) Average locomotion speed (gray trace) and the mean of all animals (black trace ± SEM) across familiarization and novel environment exploration (n = 5 animals). The average speed was measured in a 3-min time window for all animals, thus proportional to the distance traveled for each animal.

(E) Average neuronal activity relative to locomotion speed in the novel (black ± SEM; day 1 and novel day 6) and familiar (yellow ± SEM; day 5 and familiar day 6) environments (dotted lines: linear fits, normalized to the maximal response in the first bin).

(F–J) As in (A)–(E), but with Calb2-cre animals unilaterally injected with AAV5-hSyn-Flex-GCaMP6s and ventral MCs imaged in the ventral hilus.

(G) As in (B) but for ventral MC (n = 60 cells, 4 animals, ***$p < 0.001$ Wilcoxon signed-rank test).

(H) As in (C) but for ventral MC (4 animals, *$p < 0.05$; **$p < 0.01$, Kruskal-Wallis test; Dunn's multiple comparison test revealed $p = 0.01$ between day 1 and day 5, and $p = 0.02$ between day 1 and day 6).

(I and J) as in (D) and (E), but for ventral MC.

(K) Changes in mean activity (AUC) for all recorded ventral MCs during wheel running epochs in a novel or familiarized environment (n = 110 cells, n = 2 animals. ***$p < 0.001$ Wilcoxon signed-rank test).

(L) Representative traces of Ca^{2+} transients of a single cell in familiar and novel environments. Foot shock (inverted triangle) did not cause any changes in Ca^{2+} activity levels in ventral MCs.

(M) Population activity (AUC normalized to the max. AUC of Ca^{2+} transients per animal) of ventral MCs before (pre-) and after (post-) foot shock in a familiar environment and that in a novel environment (***$p < 0.001$ Mann-Whitney U-test; n = 3 mice). See also Figure S4; Video S2 and Video S3.

showed significantly reduced freezing levels in retrieval (Figure 4E) than did the mCherry-expressing control group, indicating that ventral MC activity is necessary for context-memory formation. The inhibitory DREADD manipulation of ventral MCs showed no significant changes in locomotion in novel and familiar environments in the open field and during conditioning (Figures S5B, S5C, S5G, and S5H). Because acute ablation of dorsal MCs was reported to impair context discrimination,[43] we also tested the effect of inhibitory DREADDs in dorsal MCs by using Drd2-cre mice (Figure 4A). These animals showed significantly increased freezing levels in retrieval (Figure 4E), indicating distinct roles of ventral and dorsal MCs in the acquisition of contextual memory. Although these animals also tended to increase freezing in conditioning (Figure 4D), which could affect

Please cite this article in press as: Fredes et al., Ventro-dorsal Hippocampal Pathway Gates Novelty-Induced Contextual Memory Formation, Current Biology (2020), https://doi.org/10.1016/j.cub.2020.09.074

CellPress
OPEN ACCESS

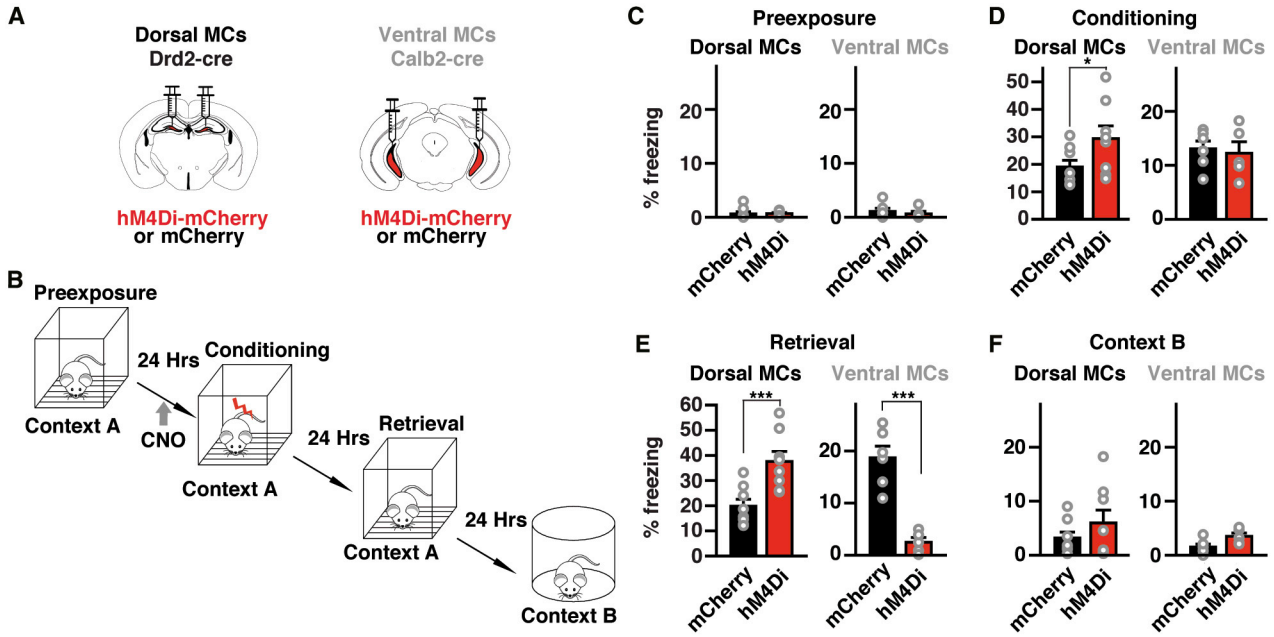

Figure 4. Differential Role of Dorsal and Ventral MCs in Context-Memory Formation

(A) Schematic representation of the injection procedure in Drd2-cre and Calb2-cre mice.

(B) Schematic representation of the behavioral paradigm.

(C–F) Freezing levels during four conditions, pre-exposure (C), conditioning (D), retrieval (E) and exposure to a novel context B (F) measured in animals expressing mCherry or hM4Di-mCherry (n = 8 Drd2-cre mice for each, and n = 6 Calb2-cre mice for each). Significant differences were detected with two-way ANOVA for Drd2-cre mice (condition [$F(3, 56) = 53.8$], $p < 0.001$; animal group ($F[1, 56] = 16.5$), $p < 0.001$; condition × animal group interaction ($F[3, 56] = 4.377$), $p < 0.01$) as well as Calb2-cre mice (condition [$F(3, 36) = 38.4$], $p < 0.001$; animal group ($F[1, 36] = 16.77$), $p < 0.001$; condition × animal group interaction ($F[3, 36] = 19.5$), $p < 0.001$). Drd2-cre mice expressing hM4Di-mCherry in dorsal MCs show a significant increase in freezing in comparison to those expressing mCherry in retrieval (**$p < 0.01$, Newman–Keuls post hoc test), whereas Calb2-cre mice expressing hM4Di-mCherry in ventral MCs show a drastic decrease in freezing (**$p < 0.01$). Drd2-cre mice expressing hM4Di-mCherry also show an increase in freezing in conditioning phase (*$p < 0.05$). See also Figure S5.

memory acquisition, the increased freezing in retrieval was context dependent (Figures 4E and 4F). The inhibitory DREADD manipulation of dorsal MCs significantly reduced locomotion in a novel environment and during conditioning (Figures S5E and S5F), which rather indicates context-independent effects of the dorsal MC activity. None of the experimental groups showed differences in comparison with control animals during pre-exposure or in a different context (Figures 4C and 4F). These results indicate that ventral MC activity, but not dorsal MC activity, is indispensable for context-memory formation.

Long-Range Axonal Projections of Ventral MCs onto Dorsal MCs Are Necessary for Contextual Memory Formation

Ventral MCs project bilaterally via long-range projection to dorsal GCs yet also have local axonal arborization within the ventral hippocampus. To conclusively determine whether the long-range projections are specifically required for context-memory formation, we perturbed synaptic transmission of ventral MC projections while animals were conditioned in a context learning paradigm (Figure 5A). For this purpose, we took advantage that hM4Di mainly blocks synaptic release at axon terminals[44] with no effect on firing rate at cell bodies, and local intracerebral injections of CNO can selectively inhibit one pathway without affecting the other collaterals.[44] By using acute slice preparation from Drd2-cre and Calb2-cre animals expressing channelrhodopsin (ChR2) and hM4Di in dorsal and ventral MCs, respectively, we confirmed that CNO (3 μM) significantly reduces light-evoked excitatory postsynaptic current (EPSC) amplitudes in dorsal GCs but not firing of ventral MCs (Figure S6). Interestingly, these experiments provided additional evidence supporting our findings in Figures 1 and 2 indicating the differential net excitatory and inhibitory roles of ventral and dorsal MCs, respectively (Figures S6D and S6E). To functionally dissect the role of axonal projections from ventral MCs during fear conditioning, we bilaterally expressed hM4Di or mCherry in ventral MCs and implanted a bilateral cannula over the dorsal DG (Figure 5B). Animals then underwent fear conditioning (Figure 5A) and received a small volume of CNO (3 mM, 300 nl) delivered directly into the dorsal DG bilaterally through the cannulas. If we administered CNO 15 min before conditioning, animals expressing hM4Di showed a robust reduction in freezing during retrieval in comparison with mCherry-expressing control animals (Figure 5E). However, infusing CNO right after conditioning or before the retrieval had no effect on freezing in comparison with controls (Figure 5E). We then tested whether inhibiting local hilar ventral MC terminals in the ventral DG altered memory acquisition by delivering CNO locally through cannulas implanted bilaterally into the ventral hilus (Figure 5B). This manipulation had no effect on freezing in comparison with control animals (Figure 5E). None of these manipulations had any significant effect on freezing levels during pre-exposure

Please cite this article in press as: Fredes et al., Ventro-dorsal Hippocampal Pathway Gates Novelty-Induced Contextual Memory Formation, Current Biology (2020), https://doi.org/10.1016/j.cub.2020.09.074

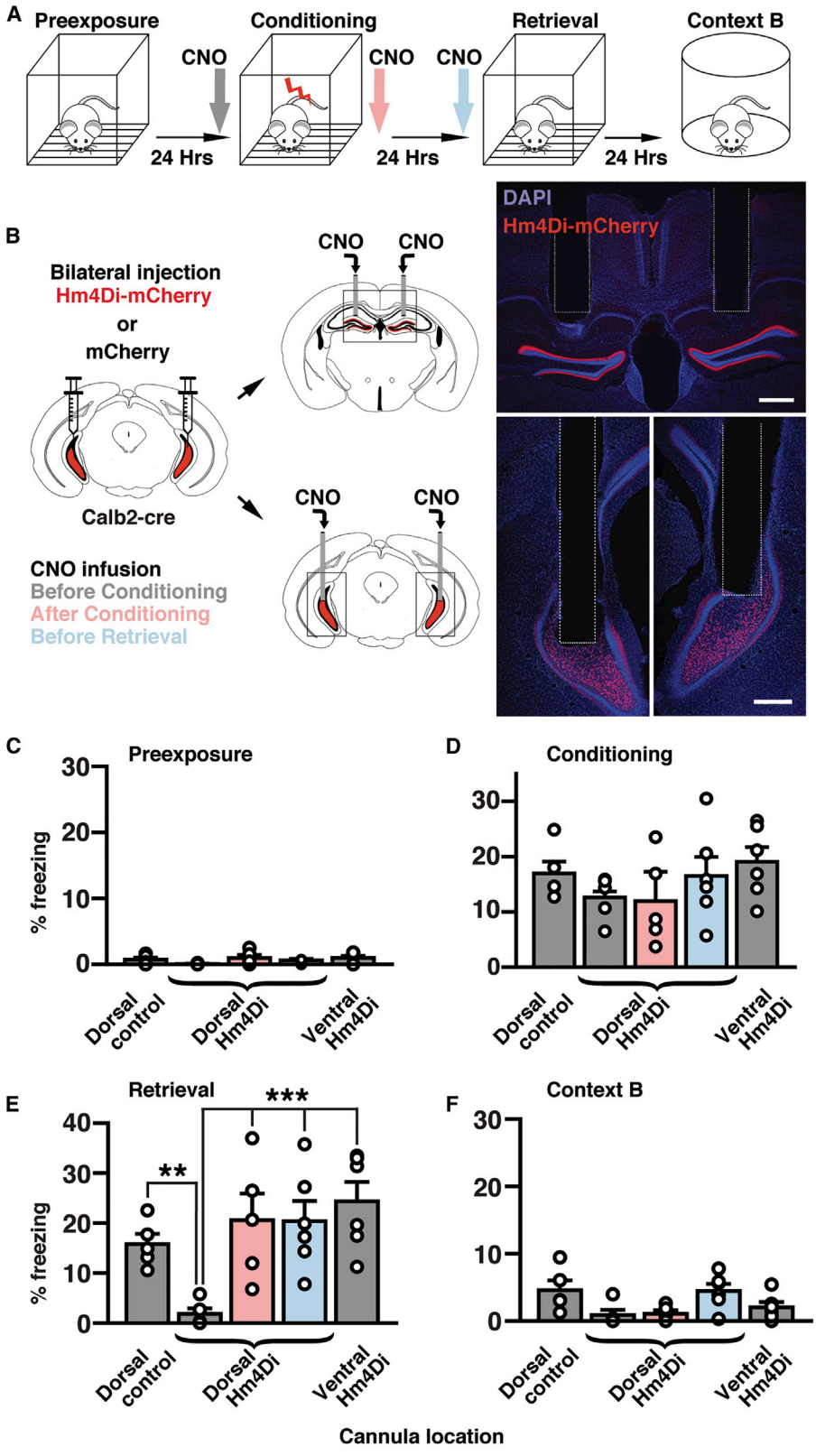

(legend on next page)

Please cite this article in press as: Fredes et al., Ventro-dorsal Hippocampal Pathway Gates Novelty-Induced Contextual Memory Formation, Current Biology (2020), https://doi.org/10.1016/j.cub.2020.09.074

CellPress
OPEN ACCESS

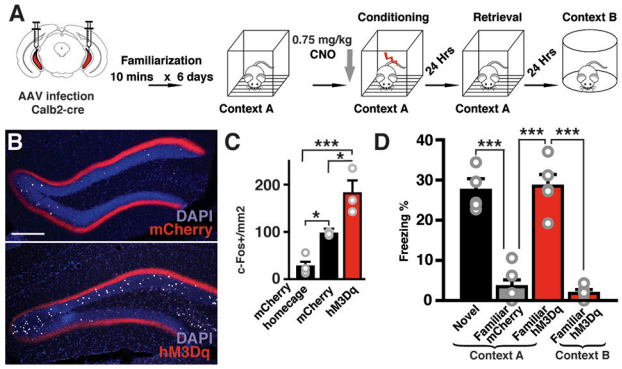

Figure 6. Activation of Ventral MCs Recovers Novelty-Induced Memory Formation

(A) Schematic representation of the familiarization fear-conditioning paradigm and ventral MC manipulation.

(B) CNO titration for memory enhancement experiments using animals injected with 0.75mg/kg of CNO before novel environment exploration. Representative confocal images of the dorsal DG of animals expressing mCherry or hM3Dq-mCherry in ventral MCs, showing c-Fos+ dorsal GCs in white. Scale bar, 200 μm.

(C) Quantification of c-Fos+ dorsal GCs (One-way ANOVA $F [2, 7] = 24.98$, $p = 0.0007$). Tukey's multiple comparison test revealed a significant increase of c-Fos+ cells in the mCherry group in comparison with the mCherry homecage control (*$p = 0.0369$). There is a further increase of c-Fos+ cells in the hM3Dq-mCherry group in comparison with the mCherry (*$p = 0.0197$) and mCherry homecage groups (***$p < 0.001$, n = 4 animals for mCherry homecage, n = 3 animals for mCherry [same data from Figures 2B and 2H], n = 3 for hM3Dq-mCherry).

(D) Effect of ventral MCs excitation by 0.75 mg/kg of CNO on freezing levels during the retrieval. Fear conditioning in a familiar environment did not cause freezing during the retrieval session (familiar mCherry), but excitation of ventral MCs restored freezing (familiar hM3Dq) to a similar level as obtained with conditioning in a novel environment (novel). This manipulation did not have any effect on freezing levels in a new environment (context B). n = 6 animals for novel, n = 5 animals for familiar mCherry and familiar hM3Dq; mean + SE, ***$p < 0.001$, one-way ANOVA with post hoc Tukey's test). See also Figure S5.

(Figure 5C), conditioning (Figure 5D), or exposure to a different environment, context B (Figure 5F). These results indicate that the activity of ventral MC terminals in the inner ML of the dorsal DG drives dorsal GC firing and is necessary for contextual memory acquisition.

Reactivation of Ventral MCs Rescues Context-Memory Formation

Environmental familiarization with extended pre-exposure is known to reduce contextual memory formation.[45,46] Thus, we hypothesized that animals in a familiar environment should form contextual memory less efficiently than in a novel one, and we tried to rescue the memory formation by activating ventral MCs. We first familiarized animals in the conditioning cage for 10 min, during six consecutive days, and then performed fear conditioning in the same cage on day 6 (Figure 6A). As expected, these animals showed significantly lower freezing levels in the retrieval session than did animals conditioned in a novel environment (Figure 6D). We next examined whether ventral MCs activation can induce contextual memory formation in a familiar environment. We bilaterally expressed hM3Dq in ventral MCs and titrated the amount of CNO (0.75 mg/kg of CNO i.p.) necessary to cause a net increase in c-Fos+ dorsal GCs (approx. 85 cells/mm^2 increase in comparison with mCherry-expressing animals) comparable to that caused by novel environment exploration in control animals (approx. 70 cells/mm^2 increase in comparison with homecage condition) (Figures 6B and 6C). Then, we bilaterally expressed hM3Dq in ventral MCs and familiarized these animals in the conditioning chamber as described before and injected 0.75 mg/kg of CNO 30 min before conditioning (Figure 6A). This manipulation did not significantly increase locomotion during conditioning (Figures S5I and S5J), but a significant increase in locomotion in a familiar open field was observed (Figure S5D). We found that freezing levels during retrieval were rescued to comparable levels of those of animals conditioned in a novel environment (Figure 6D). This rescue effect was dependent on context because no increase in freezing was observed in context B (Figure 6D). These results indicate that ventral MC activity is sufficient to form context memory in a familiar environment.

DISCUSSION

Although hippocampal novelty detection is associated with the projections from locus coeruleus (LC) to CA1 and CA3,[47,48] the mechanisms of novelty-induced activation of DG have not been yet investigated. The increase in activity of dorsal GCs seems not to be driven preferentially by medial entorhinal inputs, given that no change was observed in firing rate[29] and c-Fos+ cell numbers[30] with environmental novelty, although it is unclear whether the entorhinal cortex is not involved in detection of novelty signals under all conditions. In contrast, here we show that ventral MCs have a strong activity increase during novel environment exploration. We propose that this population activity, due to their widespread bilateral projections, can modulate the input relayed from the entorhinal cortex to dorsal GCs by globally shifting the baseline for depolarization. By this mechanism, novelty gates encoding spatial information relayed by the entorhinal

Figure 5. Ventral MC Terminal Activity in the Dorsal DG Is Indispensable for Contextual Fear Memory Formation

(A) Fear conditioning protocol. CNO was infused before conditioning (gray), after conditioning (pink), or before retrieval (blue).

(B) Calb2-cre mice were injected bilaterally with AAVs expressing hM4Di-mCherry or mCherry into the ventral hilus, and CNO was infused into the bilateral dorsal or ventral DG. Photographs (right) show examples of cannula placement. Scale bars, 500 μm.

(C–F) Percentages of freezing during four conditions: preexposure (C), conditioning (D), retrieval (E), and exposure to context B (F) were analyzed for five groups of mice, dorsal control group expressing mCherry and receiving CNO in the dorsal DG before conditioning (n = 5 animals), dorsal hM4Di groups expressing hM4Di-mCherry and receiving CNO in the dorsal DG before conditioning (gray, n = 5 animals), after conditioning (pink, n = 5 animals) or before retrieval (blue, n = 6 animals), and ventral hM4Di group expressing hM4Di-mCherry and receiving CNO in the ventral DG before conditioning (n = 6 animals). Significant differences were detected with two-way ANOVA (animal group $[F (4,88) = 6.12]$, $p < 0.001$; condition $(F [3, 88] = 60.4$, $p < 0.001$; animal group × condition interaction $(F [12, 88] = 3.05$, $p = 0.0013)$. Dorsal hM4Di group receiving CNO before conditioning shows a robust reduction in freezing in comparison with the dorsal control group (**$p < 0.01$, Newman-Keuls post hoc test) and other groups (***$p < 0.001$) in retrieval (E). No statistical differences between groups were detected during preexposure (C), conditioning (D), and exposure to context B (F). See also Figure S6.

Please cite this article in press as: Fredes et al., Ventro-dorsal Hippocampal Pathway Gates Novelty-Induced Contextual Memory Formation, Current Biology (2020), https://doi.org/10.1016/j.cub.2020.09.074

cortex, forming the engram of contextual memory in dorsal GCs. Although dorsal MCs have been shown to be involved in spatial coding, required for the discrimination of changes in local contexts in similar environments,[26,41,49,50] our results emphasize that their ventral counterparts can relay a global environmental novelty context. Such novelty also activates tyrosine-hydroxylase-expressing LC neurons, which enhances memory consolidation.[48] However, the LC and ventral MC pathways are apparently independent, because chemogenetic activation of ventral MCs is sufficient to facilitate the formation of contextual memories in familiar environments, and, contrary to the post-encoding effect of LC activation,[48] inhibition of ventral MCs after the conditioning has no effect on memory formation.

Environmental novelty increases locomotion, which could facilitate the formation of contextual memories. Interestingly, we observed an increase in locomotion in an open field during ventral MC activation (Figures S5B–S5D), though it was not observed in the contextual fear memory paradigm (Figures S5I and S5J). Thus, it is conceivable that such an increase in exploration could facilitate contextual memory formation. However, novelty signals relayed by ventral MCs do not appear to be generally linked to locomotion, as seen in those relayed by LC-CA3 pathway,[47] because both activation and inhibition of ventral MCs tended to increase locomotion in open field (Figures S5B–S5D), while they either robustly induced and suppressed context-dependent fear memory (Figures 6D and 4E). The dissociation of locomotion and contextual memory appears more evident with dorsal MC inhibition, which significantly reduced locomotion (Figures S5E and S5F) but increased contextual fear memory formation (Figure 6D). Such dissociation has also been shown with optogenetic activation of dorsal GCs during conditioning, which increases locomotion but decreases memory encoding measured by freezing during retrieval.[42] This is an interesting phenomenon that deserves a fully dedicated study.

Although the activities of dorsal GC and ventral MC are correlated during familiarization (Figures 3A–3J), the true extent of this dynamic remains an open question. This is mainly because the GRIN lens implantation injured the dendrites in the outer and middle ML and, thus, impaired the entorhinal inputs to the dorsal GCs being imaged (Figures S4C and S4D). This mechanical damage necessarily changed the dynamics of GCs and the entire dorsal DG (Figures 3F–3J). However, the inner ML and therefore ventral MCs inputs appear intact, as reflected in the robust responses of dorsal GC during ventral MC activation (Figures 2K, 2L, and 3A–3E; Video S1). Thus, these results should be carefully interpreted, because they support the correlated activity of ventral MCs and dorsal GCs during novelty exposure and familiarization but only with impaired entorhinal inputs. Despise this conundrum, altogether, our experiments emphasize that a novelty signal can be relayed via ventral MCs to the dorsal DG.

Despite the fact that novelty-induced emotional signals could also be involved in the ventral MC activation, it is striking that even electrical shock caused no activation in ventral MCs. Because novelty, by one means or another, requires the examination of memory contents,[51] our study opens intriguing new questions regarding the network computations that drive ventral MCs.

The effect of context familiarization before the conditioning (Figure 6D) looks similar to the latent inhibition, which has been described as suppression of expression rather than acquisition of associative memory by previous exposure to conditioned stimulus (CS) without unconditioned stimulus (US).[52] This view is supported by recovery of behavior reflecting memory acquisition 10–20 days after conditioned taste aversion[53] or fear conditioning using light CS paired with foot shock,[54] and those showing context-dependent performance deficit after conditioning with two to four days of CS pre-exposure.[55,56] Although these results suggest that CS-US associative memory is actually formed in the conditioning phase, it is unclear if context-US associative memory can also be formed after persistent pre-exposure to the same context. At least in most of the previous cases, ventral MCs, and probably some dorsal GCs too, should still be activated by the context in the conditioning. If so, the situation could be different in our conditioning, in which the activity of ventral MCs was greatly suppressed after six days of pre-exposure (Figure 3). Even if the acquisition took place to some extent, our rescue experiment indicates that acquisition of context-US associative memory can be strongly enhanced by the weak chemogenetic activation of ventral MCs overwhelming the effect of latent inhibition in the retrieval on day 2. How the latent inhibition works for acquisition of context-US association memory with different pre-exposure protocols is an interesting open question.

Other studies have also tested the role of ventral and dorsal MCs *in vivo* from different perspectives, employing different manipulations and spatiotemporal specificity. A recent study shows that optogenetic stimulation or inhibition of ventral MCs was able to reduce or increase the number of spontaneous epileptic seizures, respectively.[26] These results look contradictory to our data because this could imply a net inhibitory effect of ventral MCs on dorsal GCs. However, in contrast to our study, their ventral placement is directed within the intermediate DG.[8,57] In this area, there is a mixture of Calb2+ and Calb2− MCs that could result in a predominantly inhibitory net effect on the DG after MC activation. Possibly, this is the reason why the same behavioral results were obtained when manipulating the dorsal and ventral MCs populations in a novel recognition task.[26] In all our experiments, we aimed at the ventral one-third of the hilus, where the highest density of Calb2+ cells is located.[33] In another study, all MCs were permanently ablated by diphtheria toxin (DT).[43] Dorsal MCs were almost entirely ablated after one week, whereas ventral MCs died only four weeks after DT treatment. Interestingly, this perturbation changed dentate excitability and impaired contextual discrimination only during the acute but not chronic phase. This apparent recovery could be due to delayed axon sprouting of interneurons shown in the chronic phase.[43] Such slow compensatory mechanisms would not be present in acute and specific manipulation, as performed in our study. Altogether, these results indicate a clear functional separation of dorsal and ventral MCs. In particular, we have shown that inhibition of dorsal MCs causes no change in c-Fos+ dorsal GCs but causes an acute increase in freezing during conditioning. These data suggest a context-independent role of dorsal MCs in fear behavior, by a mechanism independent from dorsal GC activation, possibly through an indirect effect on hilar somatostatin-positive interneurons that project to the medial septum.[58]

Please cite this article in press as: Fredes et al., Ventro-dorsal Hippocampal Pathway Gates Novelty-Induced Contextual Memory Formation, Current Biology (2020), https://doi.org/10.1016/j.cub.2020.09.074

It has been shown that optogenetic activation of dorsal GCs during encoding leads to decreased freezing in the retrieval of contextual fear.[42] Given that we see a tendency of increase in c-Fos+ dorsal GCs in the lower blade after dorsal MC inhibition (Figure S3H), we expected that a similar decrease in freezing might occur when chemogenetically inhibiting dorsal MCs. In contrast, we observe an increase of freezing during retrieval after inhibiting dorsal MCs (Figure 4E). At least two reasons could explain these differences. First, in Kheirbek et al.[42] the entire dorsal GC population was activated in POMC-Cre/ChR2 mice. Thus, their results are not comparable with our indirect GC activation through chemogenetic inhibition of dorsal MCs. Second, our approach does not synchronize dorsal GCs activation (See Video S1), a phenomenon expected in the optogenetic approach, causing a fundamentally different network dynamic.

We have shown that contextual fear memory formation is gated by ventral MC long-range projections to the dorsal DG (Figure 5). However, ventral MCs will influence the local circuitry within the ventral DG, which could affect other types of behaviors. It has been shown that inhibiting the activity of ventral GCs confers resilience to chronic stress[59] and that ventral DG engram cells are reactivated in emotionally salient contexts.[60] Thus, a comprehensive understanding of the mechanism of contextual memory formation mediated by ventral MC activity might require a perspective on anxiety and chronic stress too.

Even though the entorhinal cortex has a role in context-memory formation,[61] there are mixed reports about its contribution to contextual fear conditioning. In one study, full medial entorhinal lesions showed no alteration in contextual fear conditioning.[62] On the other hand, rats with similar lesions showed impaired fear memory when exposed to previously visited contexts.[63] Likewise, deleting NR1 subunit of NMDA receptors in dentate GCs does not affect contextual fear conditioning using different contexts, though only very similar contexts can cause discrimination problems in the mutant mice.[64] Thus, entorhinal inputs to DG likely finetune pattern separation while acquiring contextual memory, whereas direct entorhinal input to CA3 underlies contextual memory retrieval.[64,65] However, direct optogenetic inhibition of dorsal GCs block context-memory acquisition,[16,42] which indicates that dorsal GCs firing is indispensable for context-memory formation. Consistent with this evidence, our data demonstrate that memory acquisition requires ventral MCs input to dorsal GCs. As the ventral MC projection spreads across most of the DG, we propose that ventral MC activity conveys a novelty signal that functions as gain control of dorsal GC activity during acquisition. This hypothesis is further supported by the finding that GC dendrites have voltage attenuation, which can strongly weaken entorhinal synaptic input.[66,67] Yet, ventral MC axons form synapses much closer to the GC soma than those originating from the entorhinal cortex, so they are ideally positioned to regulate action potential firing in dorsal GCs.[24]

Where is the novelty signal generated? Given that MCs primarily receive intrahippocampal inputs from within the DG and CA3,[68] it remains puzzling how these areas could contribute to generating a novelty signal in ventral MCs. However, these results are restricted mainly to dorsal and intermediate MCs. Thus, ventral MCs could have a differential network connectivity that could shed light on this question.

Our findings could contribute to a revision of existing models of hippocampal-dependent context learning by adding another independent component representing environmental novelty derived from the ventral MC activity. This novelty is distinct from that involved in the comparison between contextual information currently observed and that associated with familiar contexts used in the BACON model.[69] This new component needs long and persistent exposure to the context to reduce the novelty signal, which inhibits rather than facilitates conditionability through the process of familiarization.[69]

Numerous studies indicate that ventral and dorsal hippocampal subdivisions are functionally dissociated.[7,8,57,70,71] Our results revise this assumption and demonstrate that novelty information is relayed through a ventro-dorsal hippocampal connection—a crucial interaction for contextual-memory formation.

STAR★METHODS

Detailed methods are provided in the online version of this paper and include the following:

- KEY RESOURCES TABLE
- RESOURCE AVAILABILITY
  - Lead Contact
  - Materials Availability
  - Data and Code Availability
- EXPERIMENTAL MODELS AND SUBJECT DETAILS
- METHOD DETAILS
  - Virus vectors
  - Stereotactic injections, cannula and GRIN lens implantation
  - Calcium imaging in behaving mice and data analysis
  - Fear conditioning and novel and familiar environment exploration
  - CNO delivery
  - Imunohistochemistry and *in situ* hybridization
  - c-Fos counting
  - Electron microscopy
  - Slice electrophysiology
- QUANTIFICATION AND STATISTICAL ANALYSIS

SUPPLEMENTAL INFORMATION

Supplemental Information can be found online at https://doi.org/10.1016/j.cub.2020.09.074.

ACKNOWLEDGMENTS

We thank Peter Jonas and Peter Somogyi for critically reading the manuscript, Satoshi Kida for helpful discussion, Taijia Makinen for providing the Prox1-creERT2 mouse line, and Hiromu Yawo for the VAMP2-Venus construct. We also thank Vivek Jayaraman, Ph.D.; Rex A. Kerr, Ph.D.; Douglas S. Kim, Ph.D.; Loren L. Looger, Ph.D.; and Karel Svoboda, Ph.D. from the GENIE Project, Janelia Farm Research Campus, Howard Hughes Medical Institute for the viral constructs used for GCaMP6s expression. We also thank Jacqueline Montanaro, Vanessa Zheden, David Kleindienst, and Laura Burnett for technical assistance, as well as Robert Beattie for imaging assistance. This work was supported by a European Research Council Advanced Grant 694539 to R.S.

AUTHOR CONTRIBUTIONS

F.F. conceived the project and performed the experiments. F.F., M.J., and R.S. designed the experiments. M.A.S. performed the EM and *in situ* hybridization experiments and assisted the surgeries. P.K. performed the slice electrophysiology experiments. K.K. provided the virus AAV_1-CAG-Vamp2-Venus and AAV_{Dj}-FLEX-rev-ChR2-HA-2a-hM4Di. M.J. analyzed calcium imaging data. F.F. analyzed all the other data. F.F., M.J., and R.S. wrote the paper.

DECLARATION OF INTERESTS

All authors declare no competing interests.

Received: January 31, 2020
Revised: September 8, 2020
Accepted: September 24, 2020
Published: October 15, 2020

REFERENCES

1. Fenker, D.B., Frey, J.U., Schuetze, H., Heipertz, D., Heinze, H.-J., and Düzel, E. (2008). Novel scenes improve recollection and recall of words. J. Cogn. Neurosci. *20*, 1250–1265.
2. Kaplan, R., Horner, A.J., Bandettini, P.A., Doeller, C.F., and Burgess, N. (2014). Human hippocampal processing of environmental novelty during spatial navigation. Hippocampus *24*, 740–750.
3. Knight, R. (1996). Contribution of human hippocampal region to novelty detection. Nature *383*, 256–259.
4. Floriou-Servou, A., von Ziegler, L., Stalder, L., Sturman, O., Privitera, M., Rassi, A., Cremonesi, A., Thöny, B., and Bohacek, J. (2018). Distinct Proteomic, Transcriptomic, and Epigenetic Stress Responses in Dorsal and Ventral Hippocampus. Biol. Psychiatry *84*, 531–541.
5. Kafkas, A., and Montaldi, D. (2018). How do memory systems detect and respond to novelty? Neurosci. Lett. *680*, 60–68.
6. Buzsáki, G., and Moser, E.I. (2013). Memory, navigation and theta rhythm in the hippocampal-entorhinal system. Nat. Neurosci. *16*, 130–138.
7. Moser, M.B., and Moser, E.I. (1998). Functional differentiation in the hippocampus. Hippocampus *8*, 608–619.
8. Fanselow, M.S., and Dong, H.-W. (2010). Are the dorsal and ventral hippocampus functionally distinct structures? Neuron *65*, 7–19.
9. Kjelstrup, K.G., Tuvnes, F.A., Steffenach, H.-A., Murison, R., Moser, E.I., and Moser, M.-B. (2002). Reduced fear expression after lesions of the ventral hippocampus. Proc. Natl. Acad. Sci. USA *99*, 10825–10830.
10. Hunsaker, M.R., and Kesner, R.P. (2008). Dissociations across the dorsal-ventral axis of CA3 and CA1 for encoding and retrieval of contextual and auditory-cued fear. Neurobiol. Learn. Mem. *89*, 61–69.
11. Hunsaker, M.R., Rosenberg, J.S., and Kesner, R.P. (2008). The role of the dentate gyrus, CA3a,b, and CA3c for detecting spatial and environmental novelty. Hippocampus *18*, 1064–1073.
12. de Hoz, L., Knox, J., and Morris, R.G.M. (2003). Longitudinal axis of the hippocampus: both septal and temporal poles of the hippocampus support water maze spatial learning depending on the training protocol. Hippocampus *13*, 587–603.
13. Temple, M.D., Worley, P.F., and Steward, O. (2003). Visualizing changes in circuit activity resulting from denervation and reinnervation using immediate early gene expression. J. Neurosci. *23*, 2779–2788.
14. Sariñana, J., Kitamura, T., Künzler, P., Sultzman, L., and Tonegawa, S. (2014). Differential roles of the dopamine 1-class receptors, D1R and D5R, in hippocampal dependent memory. Proc. Natl. Acad. Sci. USA *111*, 8245–8250.
15. Liu, X., Ramirez, S., Pang, P.T., Puryear, C.B., Govindarajan, A., Deisseroth, K., and Tonegawa, S. (2012). Optogenetic stimulation of a hippocampal engram activates fear memory recall. Nature *484*, 381–385.
16. Bernier, B.E., Lacagnina, A.F., Ayoub, A., Shue, F., Zemelman, B.V., Krasne, F.B., and Drew, M.R. (2017). Dentate Gyrus Contributes to Retrieval as well as Encoding: Evidence from Context Fear Conditioning, Recall, and Extinction. J. Neurosci. *37*, 6359–6371.
17. Ramirez, S., Liu, X., Lin, P.-A., Suh, J., Pignatelli, M., Redondo, R.L., Ryan, T.J., and Tonegawa, S. (2013). Creating a false memory in the hippocampus. Science *341*, 387–391.
18. Redondo, R.L., Kim, J., Arons, A.L., Ramirez, S., Liu, X., and Tonegawa, S. (2014). Bidirectional switch of the valence associated with a hippocampal contextual memory engram. Nature *513*, 426–430.
19. Josselyn, S.A., Köhler, S., and Frankland, P.W. (2015). Finding the engram. Nat. Rev. Neurosci. *16*, 521–534.
20. Hainmueller, T., and Bartos, M. (2018). Parallel emergence of stable and dynamic memory engrams in the hippocampus. Nature *558*, 292–296.
21. Buckmaster, P.S., Wenzel, H.J., Kunkel, D.D., and Schwartzkroin, P.A. (1996). Axon arbors and synaptic connections of hippocampal mossy cells in the rat in vivo. J. Comp. Neurol. *366*, 271–292.
22. Blasco-Ibáñez, J.M., and Freund, T.F. (1997). Distribution, ultrastructure, and connectivity of calretinin-immunoreactive mossy cells of the mouse dentate gyrus. Hippocampus *7*, 307–320.
23. Fujise, N., Liu, Y., Hori, N., and Kosaka, T. (1998). Distribution of calretinin immunoreactivity in the mouse dentate gyrus: II. Mossy cells, with special reference to their dorsoventral difference in calretinin immunoreactivity. Neuroscience *82*, 181–200.
24. Scharfman, H.E. (2016). The enigmatic mossy cell of the dentate gyrus. Nat. Rev. Neurosci. *17*, 562–575.
25. Scharfman, H.E. (1995). Electrophysiological evidence that dentate hilar mossy cells are excitatory and innervate both granule cells and interneurons. J. Neurophysiol. *74*, 179–194.
26. Bui, A.D., Nguyen, T.M., Limouse, C., Kim, H.K., Szabo, G.G., Felong, S., Maroso, M., and Soltesz, I. (2018). Dentate gyrus mossy cells control spontaneous convulsive seizures and spatial memory. Science *359*, 787–790.
27. Hsu, T.-T., Lee, C.-T., Tai, M.-H., and Lien, C.-C. (2016). Differential Recruitment of Dentate Gyrus Interneuron Types by Commissural Versus Perforant Pathways. Cereb. Cortex *26*, 2715–2727.
28. Ewell, L.A., and Jones, M.V. (2010). Frequency-tuned distribution of inhibition in the dentate gyrus. J. Neurosci. *30*, 12597–12607.
29. Burgalossi, A., von Heimendahl, M., and Brecht, M. (2014). Deep layer neurons in the rat medial entorhinal cortex fire sparsely irrespective of spatial novelty. Front. Neural Circuits *8*, 74.
30. Jenkins, T.A., Amin, E., Pearce, J.M., Brown, M.W., and Aggleton, J.P. (2004). Novel spatial arrangements of familiar visual stimuli promote activity in the rat hippocampal formation but not the parahippocampal cortices: a c-fos expression study. Neuroscience *124*, 43–52.
31. Duffy, A.M., Schaner, M.J., Chin, J., and Scharfman, H.E. (2013). Expression of c-fos in hilar mossy cells of the dentate gyrus in vivo. Hippocampus *23*, 649–655.
32. Bernstein, H.L., Lu, Y.-L., Botterill, J.J., and Scharfman, H.E. (2019). Novelty and Novel Objects Increase c-Fos Immunoreactivity in Mossy Cells in the Mouse Dentate Gyrus. Neural Plast. *2019*, 1815371.
33. Cembrowski, M.S., Wang, L., Sugino, K., Shields, B.C., and Spruston, N. (2016). Hipposeq: a comprehensive RNA-seq database of gene expression in hippocampal principal neurons. eLife *5*, e14997.
34. Bermudez-Hernandez, K., Lu, Y.-L., Moretto, J., Jain, S., LaFrancois, J.J., Duffy, A.M., and Scharfman, H.E. (2017). Hilar granule cells of the mouse dentate gyrus: effects of age, septotemporal location, strain, and selective deletion of the proapoptotic gene BAX. Brain Struct. Funct. *222*, 3147–3161.
35. Gulyás, A.I., Miettinen, R., Jacobowitz, D.M., and Freund, T.F. (1992). Calretinin is present in non-pyramidal cells of the rat hippocampus–I. A new type of neuron specifically associated with the mossy fibre system. Neuroscience *48*, 1–27.

36. Toni, N., and Sultan, S. (2011). Synapse formation on adult-born hippocampal neurons. Eur. J. Neurosci. *33*, 1062–1068.

37. Johnston, S.T., Parylak, S.L., Kim, S., Mac, N., Lim, C.K., Gallina, I.S., Bloyd, C.W., Newberry, A., Saavedra, C.D., Novák, O., et al. (2020). AAV Ablates Neurogenesis in the Adult Murine Hippocampus. bioRxiv, 31:2020.01.18.911362.

38. Espinoza, C., Guzman, S.J., Zhang, X., and Jonas, P. (2018). Parvalbumin^{+} interneurons obey unique connectivity rules and establish a powerful lateral-inhibition microcircuit in dentate gyrus. Nat. Commun. *9*, 4605.

39. Puighermanal, E., Biever, A., Espallergues, J., Gangarossa, G., De Bundel, D., and Valjent, E. (2015). drd2-cre:ribotag mouse line unravels the possible diversity of dopamine d2 receptor-expressing cells of the dorsal mouse hippocampus. Hippocampus *25*, 858–875.

40. Pilz, G.-A., Carta, S., Stäuble, A., Ayaz, A., Jessberger, S., and Helmchen, F. (2016). Functional Imaging of Dentate Granule Cells in the Adult Mouse Hippocampus. J. Neurosci. *36*, 7407–7414.

41. Danielson, N.B., Turi, G.F., Ladow, M., Chavlis, S., Petrantonakis, P.C., Poirazi, P., and Losonczy, A. (2017). In Vivo Imaging of Dentate Gyrus Mossy Cells in Behaving Mice. Neuron *93*, 552–559.e4.

42. Kheirbek, M.A., Drew, L.J., Burghardt, N.S., Costantini, D.O., Tannenholz, L., Ahmari, S.E., Zeng, H., Fenton, A.A., and Hen, R. (2013). Differential control of learning and anxiety along the dorsoventral axis of the dentate gyrus. Neuron *77*, 955–968.

43. Jinde, S., Zsiros, V., Jiang, Z., Nakao, K., Pickel, J., Kohno, K., Belforte, J.E., and Nakazawa, K. (2012). Hilar mossy cell degeneration causes transient dentate granule cell hyperexcitability and impaired pattern separation. Neuron *76*, 1189–1200.

44. Stachniak, T.J., Ghosh, A., and Sternson, S.M. (2014). Chemogenetic synaptic silencing of neural circuits localizes a hypothalamus®midbrain pathway for feeding behavior. Neuron *82*, 797–808.

45. Hall, J., Thomas, K.L., and Everitt, B.J. (2000). Rapid and selective induction of BDNF expression in the hippocampus during contextual learning. Nat. Neurosci. *3*, 533–535.

46. Kiernan, M.J., and Westbrook, R.F. (1993). Effects of exposure to a to-be-shocked environment upon the rat's freezing response: evidence for facilitation, latent inhibition, and perceptual learning. Q. J. Exp. Psychol. B *46*, 271–288.

47. Wagatsuma, A., Okuyama, T., Sun, C., Smith, L.M., Abe, K., and Tonegawa, S. (2018). Locus coeruleus input to hippocampal CA3 drives single-trial learning of a novel context. Proc. Natl. Acad. Sci. USA *115*, E310–E316.

48. Takeuchi, T., Duszkiewicz, A.J., Sonneborn, A., Spooner, P.A., Yamasaki, M., Watanabe, M., Smith, C.C., Fernández, G., Deisseroth, K., Greene, R.W., and Morris, R.G. (2016). Locus coeruleus and dopaminergic consolidation of everyday memory. Nature *537*, 357–362.

49. Senzai, Y., and Buzsáki, G. (2017). Physiological Properties and Behavioral Correlates of Hippocampal Granule Cells and Mossy Cells. Neuron *93*, 691–704.e5.

50. GoodSmith, D., Chen, X., Wang, C., Kim, S.H., Song, H., Burgalossi, A., Christian, K.M., and Knierim, J.J. (2017). Spatial Representations of Granule Cells and Mossy Cells of the Dentate Gyrus. Neuron *93*, 677–690.e5.

51. Barto, A., Mirolli, M., and Baldassarre, G. (2013). Novelty or surprise? Front. Psychol. *4*, 907.

52. Polack, C.W., Jozefowiez, J., and Miller, R.R. (2017). Stepping back from 'persistence and relapse' to see the forest: Associative interference. Behav. Processes *141*, 128–136.

53. Bakner, L., Strohen, K., Nordeen, M., and Riccio, D.C. (1991). Postconditioning recovery from the latent inhibition effect in conditioned taste aversion. Physiol. Behav. *50*, 1269–1272.

54. Kraemer, P.J., Randall, C.K., and Carbary, T.J. (1991). Release from latent inhibition with delayed testing. Anim. Learn. Behav. *19*, 139–145.

55. Grahame, N., Barnet, R., Gunther, L., and Miller, R. (1994). Latent inhibition as a performance deficit resulting from CS—context associations. Anim. Learn. Behav. *22*, 395–408.

56. Miller, R.R., Laborda, M.A., Polack, C.W., and Miguez, G. (2015). Comparing the context specificity of extinction and latent inhibition. Learn. Behav. *43*, 384–395.

57. Strange, B.A., Witter, M.P., Lein, E.S., and Moser, E.I. (2014). Functional organization of the hippocampal longitudinal axis. Nat. Rev. Neurosci. *15*, 655–669.

58. Yuan, M., Meyer, T., Benkowitz, C., Savanthrapadian, S., Ansel-Bollepalli, L., Foggetti, A., Wulff, P., Alcami, P., Elgueta, C., and Bartos, M. (2017). Somatostatin-positive interneurons in the dentate gyrus of mice provide local- and long-range septal synaptic inhibition. eLife *6*, e21105.

59. Anacker, C., Luna, V.M., Stevens, G.S., Millette, A., Shores, R., Jimenez, J.C., Chen, B., and Hen, R. (2018). Hippocampal neurogenesis confers stress resilience by inhibiting the ventral dentate gyrus. Nature *559*, 98–102.

60. Chen, B.K., Murawski, N.J., Cincotta, C., McKissick, O., Finkelstein, A., Hamidi, A.B., Merfeld, E., Doucette, E., Grella, S.L., Shpokayte, M., et al. (2019). Artificially Enhancing and Suppressing Hippocampus-Mediated Memories. Curr. Biol. *29*, 1885–1894.e4.

61. Kitamura, T., Sun, C., Martin, J., Kitch, L.J., Schnitzer, M.J., and Tonegawa, S. (2015). Entorhinal Cortical Ocean Cells Encode Specific Contexts and Drive Context-Specific Fear Memory. Neuron *87*, 1317–1331.

62. Hales, J.B., Schlesiger, M.I., Leutgeb, J.K., Squire, L.R., Leutgeb, S., and Clark, R.E. (2014). Medial entorhinal cortex lesions only partially disrupt hippocampal place cells and hippocampus-dependent place memory. Cell Rep. *9*, 893–901.

63. Hales, J.B., Vincze, J.L., Reitz, N.T., Ocampo, A.C., Leutgeb, S., and Clark, R.E. (2018). Recent and remote retrograde memory deficit in rats with medial entorhinal cortex lesions. Neurobiol. Learn. Mem. *155*, 157–163.

64. McHugh, T.J., Jones, M.W., Quinn, J.J., Balthasar, N., Coppari, R., Elmquist, J.K., Lowell, B.B., Fanselow, M.S., Wilson, M.A., and Tonegawa, S. (2007). Dentate gyrus NMDA receptors mediate rapid pattern separation in the hippocampal network. Science *317*, 94–99.

65. Leutgeb, J.K., Leutgeb, S., Moser, M.-B., and Moser, E.I. (2007). Pattern separation in the dentate gyrus and CA3 of the hippocampus. Science *315*, 961–966.

66. Krueppel, R., Remy, S., and Beck, H. (2011). Dendritic integration in hippocampal dentate granule cells. Neuron *71*, 512–528.

67. Schmidt-Hieber, C., Jonas, P., and Bischofberger, J. (2007). Subthreshold dendritic signal processing and coincidence detection in dentate gyrus granule cells. J. Neurosci. *27*, 8430–8441.

68. Sun, Y., Grieco, S.F., Holmes, T.C., and Xu, X. (2017). Local and Long-Range Circuit Connections to Hilar Mossy Cells in the Dentate Gyrus. eNeuro *4*, 4:ENEURO.0097–, 2017.

69. Krasne, F.B., Cushman, J.D., and Fanselow, M.S. (2015). A Bayesian context fear learning algorithm/automaton. Front. Behav. Neurosci. *9*, 112.

70. Bannerman, D.M., Rawlins, J.N.P., McHugh, S.B., Deacon, R.M.J., Yee, B.K., Bast, T., Zhang, W.-N., Pothuizen, H.H.J., and Feldon, J. (2004). Regional dissociations within the hippocampus–memory and anxiety. Neurosci. Biobehav. Rev. *28*, 273–283.

71. Royer, S., Sirota, A., Patel, J., and Buzsáki, G. (2010). Distinct representations and theta dynamics in dorsal and ventral hippocampus. J. Neurosci. *30*, 1777–1787.

72. Bazigou, E., Lyons, O.T.A., Smith, A., Venn, G.E., Cope, C., Brown, N.A., and Makinen, T. (2011). Genes regulating lymphangiogenesis control venous valve formation and maintenance in mice. J. Clin. Invest. *121*, 2984–2992.

73. Giovannucci, A., Friedrich, J., Gunn, P., Kalfon, J., Brown, B.L., Koay, S.A., Taxidis, J., Najafi, F., Gauthier, J.L., Zhou, P., et al.

(2019). CaImAn an open source tool for scalable calcium imaging data analysis. eLife *8*, 413.

74. Parajuli, L.K., Nakajima, C., Kulik, A., Matsui, K., Schneider, T., Shigemoto, R., and Fukazawa, Y. (2012). Quantitative regional and ultrastructural localization of the Ca(v)2.3 subunit of R-type calcium channel in mouse brain. J. Neurosci. *32*, 13555–13567.

75. Vega-Zuniga, T., Trost, D., Schicker, K., Bogner, E.M., and Luksch, H. (2018). The Medial Ventrothalamic Circuitry: Cells Implicated in a Bimodal Network. Front. Neural Circuits *12*, 9.

Please cite this article in press as: Fredes et al., Ventro-dorsal Hippocampal Pathway Gates Novelty-Induced Contextual Memory Formation, Current Biology (2020), https://doi.org/10.1016/j.cub.2020.09.074

STAR★METHODS

KEY RESOURCES TABLE

REAGENT or RESOURCE	SOURCE	IDENTIFIER
Antibodies		
Rabbit polyclonal anti-calretinin	Millipore	Cat# AB5054, RRID: AB_2068506
Goat polyclonal anti c-Fos	Santa Cruz Biotechnology	Cat# sc-52-G, RRID: AB_2629503
Rabbit anti-PV	Abcam	Cat# ab11427; RRID: AB_298032
Mouse anti-RFP IgG1k	MBL	Cat# M165-3; RRID: AB_1520843
Mouse anti-GFP IgG2a (clone mFX75)	Wako	Cat# 012-22541
Rabbit anti-HA	Cell Signaling Tech.	Cat# 3724
Streptavidin Alexa Fluor 488 conjugated	Molecular Probes	Cat# S11223
Donkey anti-Rabbit IgG Alexa Fluor 488	Molecualr Probes	Cat# A-21206; RRID: AB_2535792
Donkey anti-Goat IgG Alexa Fluor 647	Molecular Probes	Cat# A-21447; RRID: AB_141844
Bacterial and Virus Strains		
AAV_5-hSyn-DIO-mCherry	Addgene	RRID: Addgene_50459
AAV_5-hSynDIO-hM4D(Gi)-mCherry	Addgene	RRID: Addgene_44362
AAV_5-hSyn-DIO-Hm3Dq-mCherry	Addgene	RRID: Addgene_44361
AAV_9-hSyn-Flex-GCaMP6s-WPRE-SV40	U Penn Vector Core	N/A
AAV_5-hSyn-Flex-GCaMP6s-WPRE-SV40	U Penn Vector Core	N/A
AAV_1-CAG-Vamp2-venus	Kenta Kobayashi	N/A
AAV_2-CAG::FLEX-rev::ChR2-HA-2a-hM4D	Addgene	RRID: Addgene_52521
Chemicals, Peptides, and Recombinant Proteins		
Tamoxifen	Sigma	Cat# T5648
Clozapine-N-oxide, CNO	Tocris	Cat# 4936
Critical Commercial Assays		
RNAscope Fluorescent Multiplex Assay	https://acdbio.com/products	Cat# 320850
Experimental Models: Organisms/Strains		
Mouse: Calretitnin-cre; Calb2-IRES-Cre	The Jackson Laboratory	JAX: 010774
Mouse: Drd2-cre (B6.FVB (Cg)-Tg (Drd2-cre) ER44Gsat/Mmcd	MMRRC Repository	RRID: MMRRC_017263-UCD
Mouse: Prox1-creERT2	Bazigou et al.[72]	N/A
Mouse: vGAT-ChR2-EYFP; Tg(Slc32a1-COP4*H134R/EYFP)8Gfng	The Jackson Laboratory	RRID: IMSR_JAX:014548
Software and Algorithms		
ImageJ	https://imagej.net/	RRID: SCR_003070
MATLAB	http://www.mathworks.com/products/matlab/	RRID: SCR_001622
GraphPad Prism	http://www.graphpad.com/	RRID: SCR_002798
Deposited Data		
Raw data for figures	https://doi.org/10.17632/p2spfxzf57.1	N/A

RESOURCE AVAILABILITY

Lead Contact

Further information and requests for resources and reagents should be directed to and will be fulfilled by the Lead Contact, Ryuichi Shigemoto (ryuichi.shigemoto@ist.ac.at)

Materials Availability

This study did not generate any new reagents or mouse lines.

Data and Code Availability

Original data have been deposited to Mendeley Data:
https://doi.org/10.17632/p2spfxzf57.1

EXPERIMENTAL MODELS AND SUBJECT DETAILS

Mouse protocols were reviewed by the institutional preclinical core facility (PCF) at IST Austria. All breeding and experimentation were performed under a license approved by the Austrian Federal Ministry of Science and Research in accordance with the Austrian and EU animal laws. Male mice C56BL6/J, Calb2-cre (JAX 010774), Drd2-cre (B6.FVB (Cg)-Tg (Drd2-cre)ER44Gsat/Mmcd, MMRRC), vGAT-ChR2-EYFP (JAX 014548) and Prox1-creERT2, developed by Taijia Makinen[72] were all on a C56BL6/J background and 2 to 8 months old for use in this study. Littermates were housed together before surgery. Animals received food and water *ad libitum* and were housed under a 12 h light-dark cycle. Littermates were randomly allocated to experimental groups. After surgery animals were housed individually and allowed to recover for at least 3 weeks before experiments.

METHOD DETAILS

Virus vectors

AAV_5-hSyn-DIO-mCherry, AAV_5-hSynDIO-hM4Di-mCherry and AAV_5-hSyn-DIO-hM3Dq-mCherry vectors were obtained from University of North Carolina vector core and Addgene viral service. AAV_9-hSyn-Flex-GCaMP6s-WPRE-SV40 and AAV_5-hSyn-Flex-GCaMP6s-WPRE-SV40 were obtained from University of Pennsylvania Vector Core. $pAAV_1$-CAG-Vamp2-venus transfer plasmid was generated by subcloning VAMP2-venus gene cassette obtained from Hiromu Yawo into pAAV-CaMKII-GFP (Addgene). Plasmid AAV-CAG::FLEX-rev::ChR2-HA-2a-hM4D was obtained from Addgene. Viral titrations were between 8×10^{12} and 7.5×10^{13} genome copy per ml. For inducing expression in Prox1-creERT2 animals, tamoxifen (T5648, Sigma) previously diluted in corn oil was injected i.p. (75 mg/kg body weight) for 5 consecutive days.

Stereotactic injections, cannula and GRIN lens implantation

Animals were anaesthetized using a mixture of 100 mg kg^{-1} Ketamine / 10 mg kg^{-1} Xylazine and injected 200 mg kg^{-1} of Novalgin as an intraoperative analgesic. Animals were placed in a stereotaxic apparatus (Kopf). The skull was exposed and craniotomies were performed at the following coordinates: ventral hilus injections or GRIN lens/cannula implantation; anteroposterior (AP) −3.2 mm, ± 3.0 mm mediolateral (ML), dorsal dentate gyrus injections or GRIN lens/cannula implantation; −1.8 mm AP and ± 1.3 mm ML. Virus injections were performed at a controlled rate of 0.1 μl min^{-1} using a water filled glass micropipette coupled to a 1 μl Hamilton microsyringe (7001; Hamilton). The pipette was slowly lowered to the target site and remained in place for another 5 min post-injection before being slowly withdrawn. For ventral hilus injections, 0.5 μl of undiluted virus was delivered at two dorso-ventral (DV) coordinates measured from the dura DV = −3.5 mm and DV = −3.7 mm. For dorsal dentate gyrus 0.7 μl of AAV_9-hSyn-Flex-GCaMP6s-WPRE-SV40 diluted 1:7 in PBS was injected at DV = −1.9 mm below the dura. For mice used in intracerebral CNO infusions, bilateral guide cannulas were implanted above the dorsal dentate gyrus (−1.7 mm AP; ± 1.0 mm ML; −1.7 mm DV) or two unilateral cannulas (PlasticsOne) were implanted above the ventral hilus on each hemisphere (−3.2 mm AP; ± 3.1 mm ML; −3.2 mm DV). For GRIN lens (DORIC lenses, Quebec) implantation four M1 screws were secured into the skull at the anterior and posterior edges of the surgical site to anchor the implant. After drying the surface of the skull, the lens was lowered slowly into the target, while imaging until the desired fluorescence was achieved. All cannulas and GRIN lens were secured to the skull using Super-bond dental cement (Sun medical, Japan). After surgery animals were injected with 5 mg kg^{-1} of Metacam (meloxicam) subcutaneously as a postoperative anti-inflammatory and painkiller. The animals recovered in a heat pad and then transferred to their home-cages and monitored closely for any discomfort signals for the three following days. Due to the short working distance of the lens (80 μm), the dorsal GRIN lens implantation required a slight "push" of the outer and medial molecular layer to reach focus. We are aware that this could impinge damage over the GCs dendrites and fibers coming from the entorhinal cortex. Although we cannot exclude any damaging effect of the GRIN lens implantation, the reproducibility of our results, the preserved functional connectivity observed with the combined chemogenetic approach, and the normal sparse activity during environmental exploration indicate that any damage is not significant for the purpose of our study.

For the case of Figure 2J, in order to avoid expression of hM3Dq-mCherry in ventral CGs of the double transgenics Prox1CreERT2/Calb2-Cre, we first injected the virus carrying GCaMP6s into the dorsal DG. For the next 5 days, these animals received tamoxifen injections to allow the recombination and expression of GCaMP6. Two weeks later when the tamoxifen effect had been gone, we injected the virus carrying hM3Dq into the ventral hilus, during the same surgery for GRIN lens implantation.

Calcium imaging in behaving mice and data analysis

Recording sessions began 4 to 6 weeks after lens implantation. First, animals were adapted to the manipulation procedure and to carrying the microscope on their heads in their home-cages for 4 days. Once adapted they explored a square environment (35 cm × 35 cm) constructed of 40 cm high matt black painted walls, visual cues in one (colored tape) and removable floor (laboratory surface paper) for 20 min every day for 6 days. Three videos of 3 min each were taken at 0, 5 and 10 min after the beginning of the exploration. The analysis was performed for the first exploration period to be consistent with the times where the foot-shock was delivered

Please cite this article in press as: Fredes et al., Ventro-dorsal Hippocampal Pathway Gates Novelty-Induced Contextual Memory Formation, Current Biology (2020), https://doi.org/10.1016/j.cub.2020.09.074

in the subsequent fear conditioning experiments. During that time animals explored the novel and familiar environments in a similar fashion, the well-known reduction of locomotion along familiarization becomes evident only after that period. The paper floor remained in the environment during all familiarization sessions for each animal to keep their individual odor constant. On day 6, after exploring the familiar environment, animals were transferred to a different environment: a square box (20 cm × 20 cm) with two white and two vertical black and white striped walls. The floor had stainless steel rods of 5 mm diameter, separated by 1 cm. Animals explored this environment for 10 min. Two videos of 3 min each were recorded during this time. Environments were carefully cleaned with 70% ethanol between animals. For familiarization in the fear conditioning environment, animals explored the conditioning cage (17 × 17 cm, Ugo Basile SLR, Italy) for 10 min for 6 consecutive days. The cage was not cleaned in order to keep their individual odor constant. After the 10 min exploration during day 6, a single foot-shock 1 sec, 0,65 mA was delivered. Immediately after, animals explored a novel environment (circular environment 20 cm diameter, 40 cm walls). For the running wheel experiments, animals were housed with a running wheel after implantation. For familiarization, animals visited a square environment (35 cm × 35 cm) constructed of 40 cm high matt black painted walls, visual cues in one (colored tape) and removable floor (laboratory surface paper) including their running wheel for 20 min every day for 6 days. On day 6, after exploring the familiar environment, animals were transferred to a different environment: a circular environment (40 cm diameter) constructed of 40 cm high matt black painted wall, visual cues (colored tape) and white plastic floor, together with their running wheel. Calcium-imaging data was acquired at 20 Hz, constant excitation power and exposure to compare fluorescent changes across sessions and corrected for motion artifacts using DORIC Neuroscience Studio Software. The rare artifacts that could not be corrected were excluded from the analysis. Imaged fields of views were highly constant across days. Regions of interest from single cells were carefully drawn by hand based on videos taken on different recording days (Figure S4B&F). To denoise and estimate the most likely neuronal activity underlying the imaged traces, we used Markov Chain Monte Carlo method developed for spike inference in continuous time (MCMC-method) provided in the CaImAn toolbox.[73] We subsequently used this inference to generate the estimated calcium traces (Figure S4I&J). This approach is more precise than other denoising approaches and inherently defines uncertainty in all inferred transients. To compare the relative change across days, we normalized all inferred events for every drawn ROI across all days to the single maximum inferred $\Delta F\ (t)/F_0$ measured for each ROI. We then calculated the area under the curve (AUC) (as a measure of neuronal activity for the first three minutes during exploration of either familiar or novel environments. We took advantage of the inherent uncertainty estimation of the MCMC-analysis to determine which events are significant. AUCs were calculated for all sessions and ROIs. We identified a total of 229 independently active dorsal granule cell ROIs and 60 ventral mossy cell ROIs for the familiarization experiment. For visualization purposes, we normalized all AUCs to the maximal AUC measured of all cells (Figure 3B&G, Figure S4O-Q). To compare the global activity change across animals, we compared the average AUC for all cells per animal (Figure 3C&H). All traces were normalized to the maximal average AUC measured across days. Inter-event intervals and peak distribution were extracted from the MCMC inferred traces. Peaks were required to have at least 1% (from normalized maximum for each ROI) (Figure S4K-N). The same analysis was performed for the experiments in which dorsal GC were imaged during chemogenetic ventral MCs activation (n = 386 dorsal GC ROIs). Control (mCherry) and experimental (hM3Dq) animals were continuously recorded after CNO injection. A strong wave of neuronal activity (Figure 2K-L, Video S1) was recorded only in experimental animals 30-33 min after injection. As exemplified in Video S1, animals showed a normal behavior after CNO, except for one animal that showed signs of seizure after 60 min of CNO injection. This behavioral abnormality did not influence the results since these time points were not included in the analysis. To extract the locomotion from the behavioral videos, a custom written MATLAB (Mathworks) script was used to contrast enhance, background subtract and fit an ellipsoid on the tracked mouse. The center of mass of the ellipsoid was used as the tracking point (see Supplementary Videos – red square on mice) (Figure 3D, I, Figure S5K, L). We separately calculated the distribution of locomotion speeds for novel (data from day 1 and day 6 novel) and familiar (data from day 5 and day 6) environments in ventral MCs and dorsal GC recorded animals, respectively. To correlate locomotion and neuronal activity, we used all AUC events, including epochs of no activity, calculated for each ROI and binned them for different locomotion speeds. All novel (day 1 and day 6 novel) and familiar (day 5 and day 6) events were used (Figure 3E, J). For the running wheel analysis, only AUC during constant locomotion on the running wheel were used (seven epochs with a total duration of 153 s and 400 s for novel and familiar environments, respectively) (Figure 3K).

Fear conditioning and novel and familiar environment exploration

Animals were acclimated to handling for three days before behavioral assays. A fear conditioning system (Ugo Basile SLR, Italy), coupled to Ethovision software (Noldus, Wageningen) was used for contextual fear conditioning and analysis. During pre-exposure, animals explored the conditioning chamber for 3 min. 24 h later, animals were reintroduced to the conditioning cage explored for 3 min. Then, three consecutive 1 s foot shocks of 0.65 mA with a 1 min interval between them were delivered. 24 h later, animals were placed again in the conditioning chamber for a 3 min exploration period. 24 h later, animals explored a distinct novel environment B, which consisted of an opaque black painted plastic tube of 35 cm diameter and 40 cm high. This environment was located in a different soundproof box than the conditioning chamber. Before every context exploration, the conditioning chamber was odorized with 1% acetic acid, and context B was odorized with 0.25% benzaldehyde. Both environments were carefully cleaned with ethanol 70% after every exploration. For conditioning in a familiar environment, animals explored the conditioning cage (17 × 17 cm, Ugo Basile SLR, Italy) for 10 min for 6 consecutive days. In order to keep the animal's individual odor constant, a piece of laboratory paper was kept under the grid floor during all the familiarization and conditioning procedures. During day 6, animals received 0.75 mg/kg of CNO i.p. and returned to their home cages for 40 min. Then, animals explored the conditioning box for 10 min. After this period, three consecutive 1 s foot shocks of 0.65 mA with a 1 min interval between them were delivered. 24 h later, animals explored the

Please cite this article in press as: Fredes et al., Ventro-dorsal Hippocampal Pathway Gates Novelty-Induced Contextual Memory Formation, Current Biology (2020), https://doi.org/10.1016/j.cub.2020.09.074

conditioning box for 3 min and 24 h later, they explored a novel environment (circular environment 20 cm diameter, 40 cm high) for 3 min. Freezing was measured with activity tracking in Ethovision, with a threshold of 500 ms for immobility detection. For measuring locomotion in familiar environments (Figure S5C, D, I, J), animals explored a circle (38.5 cm diameter) with black wall (Figure S5C) or a square (40 cm × 40 cm) with white wall (Figure S5D) for 10 min every day for 5 days before measuring distance traveled for 5 min in the same environments on day 6. The distance traveled in the circle (38.5 cm diameter) for 5 min on day 1 was used as locomotion in a novel environment (Figure S5B). For novel environment exploration and following perfusion for c-Fos immunolabelling, animals were handled for 3 days before experiments to acclimatize to the experimenter and procedures. After CNO injection, animals were kept in their home-cages for 40 min before being transferred to a square box of 20 cm by 20 cm, with two white walls, and two walls with vertical black and white lines with white plastic floor. Inside the cage there was a running wheel and a styrofoam box 5 cm by 7 cm and 3 cm high. Animals explored this environment for 30 min, then returned to their home-cage and remained there for another 40 min before perfusion.

CNO delivery

Clozapine-N-oxide (CNO, Tocris, Catalog number 4936) was dissolved in dimethylsulfoxide (DMSO) at 1% final concentration, and then diluted with PBS to 1 mg/mL for intraperitoneal (i.p.) injections and with ACSF at 3 μM for intracerebral infusions. For i.p. injections, we delivered 3 mg/kg or 0.75 mg/kg of CNO, followed by behavior 40 min after the injection. For intracranial delivery, CNO was infused bilaterally into the dorsal or ventral dentate gyrus with 0.3 μl per hemisphere at a concentration of 3 μM using a 26-gauge stainless steel internal cannula (PlasticsOne). The internal cannula was connected with a 1 μl Hamilton syringe (7001; Hamilton) to control the injection rate at 100 nL min^{-1}. The injection cannula was left connected for 5 min before removal to allow for diffusion. Finally, all behavior was performed 15 min following the drug infusion.

Imunohistochemistry and *in situ* hybridization

For immunohistochemistry, mice were overdosed with 750–1000 mg kg^{-1} mixture of Ketamine, Xylazine and perfused transcardially with PBS, followed by 4% cold paraformaldehyde (PFA) in PB. Extracted brains were kept in 30% sucrose in PB at 4°C overnight, then transferred to PBS. A sliding microtome (Leica SM2000R) was used to cut 40-μm coronal slices in PBS. Slices were washed with PBS-T (PBS + 0.2% Triton X-100), then incubated with PBS-T + 20% normal donkey serum, at room temperature for 1 h for blocking. Then, slices were incubated with one or more primary antibodies at 4°C for 24 h (rabbit anti-calretinin AB5054, Millipore, dilution 1:1000; goat anti c-Fos SC-52, Santa Cruz Biotechnology, dilution 1:500; rabbit anti-PV, Abcam, dilution 1:1000; or for electrophysiology slices, Streptavidin Alexa Fluor 488 conjugated (1:1000); rabbit anti HA-tag AB3724, Cell Signaling Technology, dilution 1:1000). Three washes of PBS-T for 10 min each were performed on the slices before 1 h incubation with secondary antibody at 1:1000 dilution (A-21206; A-21447, ThermoFisher Scientific). Slices were washed three more times in PBS-T for 10 min each, stained with 4′,6-diamidino-2-phenylindole (DAPI) to label cell nuclei and mounted with Prolong antifade reagent (Thermofisher) onto microscope slides. For *in situ* hybridization, Calb2-cre animals were injected hilus with $pAAV_5$-hSynDIO-mCherry in the ventral hilus. Three weeks later, they were anesthetized with isofluorane, decapitated and their brains removed immediately. The ventral hippocampus was dissected, placed in a Cryomold (Sakura, Japan) filled with O.C.T. Tissue-Tek compound (Sakura, Japan), and stored at −80 °C until 14 μm sections were cut with a cryostat (Microm HM 560, Thermo) and mounted in Superfrost plus slides (Thermo scientific). The whole *in situ* hybridization procedure was performed with and according to the protocol of the RNAscope Fluorescent Multiplex Assay (ACD) using probes for vGluT1 and mCherry. Slides were imaged in an upright Zeiss LSM 700 confocal microscope. Cytoarchitecture borders for cell counting were defined in accordance with the Allen Brain Institute Atlas, http://atlas.brain-map.org.

c-Fos counting

For counting c-Fos-positive granule cells in the dentate gyrus, three 40 μm sections were taken from dorsal DG and three for ventral DG from each animal if required. These sections were separated by 160 μm, thus representing the different antero-posterior levels of the whole dorsal or ventral DG. Note: the apparent reduced number of c-Fos positive GCs in control conditions compared to other studies is due to the thin sections used. This was required because after the activation experiments of ventral MCs, the high number of c-Fos positive GCs would make thicker sections uninterpretable. Pictures were taken in an upright Zeiss LSM 700 confocal microscope with the same magnification, laser power and exposure times. Then, the total area of the granule cell layer was measured, and cells positive for c-Fos within this area were counted using Fiji (https://fiji.sc). Finally, the density of cells was calculated dividing the number of cells by the area.

Electron microscopy

Animal anesthetization, fixation and pre-embedding immunoelectron microscopy (EM) were performed as described previously.[74] Briefly, mice were deeply anesthetized and trans-cardially perfused at a flow rate of 7 mL/min, first with 25 mM PBS for 1 min, followed by 10 min of fixative containing 4% paraformaldehyde, 15% picric acid and 0.05% glutaraldehyde in 0.1 M PB. Brains were removed and kept in PB until coronal sections of 50 μm thickness were cut in a vibratome (Linear Slicer Pro7, D.S.K, Japan). Slices were washed in PB twice, cryo-protected, and freeze-thawed before adding blocking solution (10% NGS in 2% BSA) for 90 min. Double immunolabeling was done by mixing primary antibodies in 2% BSA, incubated for 3 nights at 4°C. For the ventral mossy cell samples, we mixed rabbit anti-PV (1:1000, Abcam) with mouse anti-RFP IgG1k (1:1000, MBL). For the dorsal mossy cell samples, we mixed rabbit anti-PV (1:1000, Abcam) with mouse anti-GFP IgG2a (1:3000, Wako). After washing, sections were incubated overnight

Please cite this article in press as: Fredes et al., Ventro-dorsal Hippocampal Pathway Gates Novelty-Induced Contextual Memory Formation, Current Biology (2020), https://doi.org/10.1016/j.cub.2020.09.074

at 4°C in a mixture of secondary antibodies, 1.4 nm gold conjugated goat anti-rabbit (1:200, Nanoprobes) and goat anti-mouse IgG1k biotinylated (1:400, Life Technologies) antibodies for ventral mossy cell samples, and goat anti-mouse IgG2a biotinylated (1:10000, Life Technologies) antibodies for dorsal mossy cell samples. After 10 min post-fixation in 1% glutaraldehyde we performed silver enhancement of immunogold particles (HQ Silver enhancement kit, Nanoprobes) and immunoperoxidase reaction, followed by 15 min fixation with 0.5% osmium tetroxide and counterstaining with 1% uranylacetate for 30 min. Slices were dehydrated in an ascending ethanol series, propylene oxide and then infiltrated in resin (Durcupan ACM, Sigma) at room temperature overnight. Slides were flat-embedded and resin was polymerized for 48 h at 60°C. We have chosen the areas to be examined by the presence of the PV+ dendrites that were located in the inner one third of the molecular layer in a middle part of the upper blade of the dorsal dentate gyrus. The selected regions were re-embedded, and ultrathin serial sections at 70 nm thickness were cut with an ultramicrotome (Leica EM UC7) for examination in a transmission electron microscope (Tecnai 10, Philips, the Netherlands). The vast majority of DAB-positive synapses were made on GCs spines (Table S1, > 97% for ventral MCs, > 92% for dorsal MCs: Note that these values are minimum estimates because we targeted PV+ dendrites, making positive biases for synapses made on these dendrites over those on GCs) as described previously.[22] We used a total number of 450 sections covering a total examined area of 16,700 mm^2. To estimate the relative contribution of ventral and dorsal MCs to synaptic innervation onto PV+ dendrites and GCs spines, we first calculated % of DAB-positive synapses in all synapses made on PV+ dendrites examined, and % of DAB-positive synapses in all synapses made on GCs spines in surrounding areas with similar depth from the section surface (Table S1). Then, these % values on PV+ dendrites were normalized by the % values on GCs spines in each animal to calculate an index Ip/g (Table S1), which indicates innervation strength on PV+ dendrites relative to that on GCs by MCs. The Ip/g values are independent of the fraction of transfected MCs. We compared Ip/g values between ventral and dorsal MCs samples with Student's t test (n = 4 animals for each).

Slice electrophysiology

Calb2-cre and Drd2-cre mice (4.4 to 12 months old) were injected bilaterally with AAV expressing hM4Di and ChR2 in a Cre dependent manner. Three weeks post-injection they were anesthetized via i.p. injection of ketamine/xylazine (ketamine: 100 mg/kg; xylazine 10 mg/kg) and transcardially perfused with oxygenated (95% O_2 / 5 % CO_2) ice-cold artificial cerebrospinal fluid (ACSF) containing (in mM): 118 NaCl, 2.5 KCl, $MgSO_4$ 1.5, $NaH_2PO_4$1.25, $CaCl_2$ 2, Myo-inositol 3, Glucose 10, Sucrose 40, $NaHCO_3$ 25, pH = 7.4. The brain was rapidly excised and placed in a cutting chamber. Coronal brain slices were prepared with a D.S.K. Linear Slicer Pro7 (Dosaka, Japan) at 250 – 350 μm thickness for recordings of ventral MCs. For recordings of optogenetically evoked currents in dorsal GCs, parasagittal slices were prepared at a 15-20°C angle and at 1 – 1.5 mm thickness.[75] Slices were left to recover for 20 min at 35°C, thereafter heating was turned off and slices recovered to room temperature over the course of one h. One slice was transferred to the recording chamber and superfused with recording ACSF (2 mM $CaCl_2$) at a rate of 2-4 mL/min. Whole-cell patch clamp recordings were performed using an EPC 10 USB amplifier with PatchMaster software (HEKA) at a sampling rate of 20 – 50 kHz and filtered at 2.9 kHz. MCs or dentate gyrus GCs were identified morphologically. Patch pipettes were pulled with a Model P-97 horizontal puller (Sutter Instrument, USA) at a resistance of 3 – 5 MΩ and filled with internal solution containing (in mM): K-Gluconate 140, $MgCl_2$ 2, HEPES 10, EGTA 0.5, MgATP 2, NaGTP 0.2, Sucrose 32, pH = 7.4 adjusted with KOH. In addition, 0.25 - 0.3% biocytin was added to the internal solution for labeling of recorded neurons after slice fixation (4% paraformaldehyde). For optogenetic experiments, blue light (465 nm) was emitted from an LED (Plexon) and transmitted onto the slice through an optical fiber. Light pulses (5 ms duration, 15 mW) were applied at 10 Hz (for 10 s at 30 s interval) for current clamp experiments in MCs and at 0.1 - 0.5 Hz for voltage-clamp experiments in dorsal GCs. In voltage-clamp experiments, cells were held at −70 mV and light-evoked synaptic currents were measured by averaging traces of 50 - 100 light-stimulations before and 3 - 10 min after the start of the application of 3 μM CNO. To test the effect of hM4Di activation on light-evoked action potential firing, cells were hyperpolarized (~-60-70 mV) to minimize spontaneous firing. Series resistance was monitored throughout all measurements and recordings with changes in series resistance exceeding 20% were discarded. Electrophysiological data was analyzed using Patchmaster software (HEKA), Clampfit 10 (Molecular Devices) and Prism 6 (GraphPad).

QUANTIFICATION AND STATISTICAL ANALYSIS

No statistical methods were used to predetermine sample size because means, variances and effect sizes were not predictable prior to performing the experiments. Thus, we decided to use 5-8 animals for behavioral experiments according to the number of animals commonly used for similar studies. The investigators were not blind to group allocation. Data were analyzed by MATLAB (Natick, MA) for calcium imaging or by Prism 6 (GraphPad Software, La Jolla, CA) for synapse counting, c-Fos counting, and fear conditioning. Unpaired two-tailed t tests, one-way ANOVA with Tukey's post hoc test, two-way ANOVA with Newman–Keuls post hoc test, Mann-Whitney U-test, Wilcoxon signed-rank test, Kruskal-Wallis test with post hoc Dunn's multiple comparison test were used where appropriate. All statistical analyses are reported in figure legends. Significance was defined as p values < 0.05.